Optokinetic Eye Movements Elicited by Radial Optic Flow in the Macaque Monkey

MARKUS LAPPE, MARTIN PEKEL, AND KLAUS-PETER HOFFMANN
Department of Zoology and Neurobiology, Ruhr University Bochum, D-44780 Bochum, Germany

Lappe, Markus, Martin Pekel, and Klaus-Peter Hoffmann. Optokinetic eye movements elicited by radial optic flow in the macaque monkey. *J. Neurophysiol.* 79: 1461–1480, 1998. We recorded spontaneous eye movements elicited by radial optic flow in three macaque monkeys using the scleral search coil technique. Computer-generated stimuli simulated forward or backward motion of the monkey with respect to a number of small illuminated dots arranged on a virtual ground plane. We wanted to see whether optokinetic eye movements are induced by radial optic flow stimuli that simulate self-movement, quantify their parameters, and consider their effects on the processing of optic flow. A regular pattern of interchanging fast and slow eye movements with a frequency of 2 Hz was observed. When we shifted the horizontal position of the focus of expansion (FOE) during simulated forward motion (expansional optic flow), median horizontal eye position also shifted in the same direction but only by a smaller amount; for simulated backward motion (contractional optic flow), median eye position shifted in the opposite direction. We relate this to a change in Schlagfeld typically observed in optokinetic nystagmus. Direction and speed of slow phase eye movements were compared with the local flow field motion in gaze direction (the foveal flow). Eye movement direction matched well the foveal motion. Small systematic deviations could be attributed to an integration of the global motion pattern. Eye speed on average did not match foveal stimulus speed, as the median gain was only ~0.5–0.6. The gain was always lower for expanding than for contracting stimuli. We analyzed the time course of the eye movement immediately after each saccade. We found remarkable differences in the initial development of gain and directional following for expansion and contraction. For expansion, directional following and gain were initially poor and strongly influenced by the ongoing eye movement before the saccade. This was not the case for contraction. These differences also can be linked to properties of the optokinetic system. We conclude that optokinetic eye movements can be elicited by radial optic flow fields simulating self-motion. These eye movements are linked to the parafoveal flow field, i.e., the motion in the direction of gaze. In the retinal projection of the optic flow, such eye movements superimpose retinal slip. This results in complex retinal motion patterns, especially because the gain of the eye movement is small and variable. This observation has special relevance for mechanisms that determine self-motion from retinal flow fields. It is necessary to consider the influence of eye movements in optic flow analysis, but our results suggest that direction and speed of an eye movement should be treated differently.

INTRODUCTION

Whenever an animal moves, a characteristic pattern of visual motion arises, which is called the optic flow field. In the most simple case of a forward movement and a constant direction of gaze (with respect to the direction of travel), all visual motion flows out from the focus of expansion (FOE) (Gibson 1950). Such a radial flow pattern could be used to find the movement direction of the observer simply by detecting the location of the FOE (Gibson 1950; Warren et al. 1988).

Besides this use of optic flow for the guidance of self-motion, however, a further concern is its implication for visual stability and the generation of eye movements. Usually in primates an abundance of eye movements is performed during any particular behavioral task to obtain essential visual information. Objects of interest have to be fixated and, if moving, tracked with the eyes to stabilize the image of the object on the retina and allow precise identification. Self-motion, on the other hand, tends to disturb the stability of the retinal image by inducing optic flow. Reflectory eye movements such as the vestibulo-ocular reflex and the optokinetic reflex have evolved to stabilize the retinal image during self-motion (Miles and Busettini 1992). Such eye movements, on the other hand, have implications for the analysis of the optic flow field. In the retinal projection of the optic flow field, eye movements superimpose additional visual motion, which adds a rotational component to the flow field vectors (Warren and Hannon 1990). Depending on the structure of the visual scene and on the type of eye movement, the retinal flow field can differ greatly from the simple radial structure of the optic flow (Lappe and Rauschecker 1995; Regan and Beverly 1982; Warren and Hannon 1990) so that a simple search for the FOE is no longer possible for heading detection.

Humans can perform the task of heading detection from optic flow very precisely in the absence of eye movements (Warren et al. 1988). Lower, but still good accuracy, is obtained when subjects judge the heading direction from optic flow while they conduct smooth pursuit eye movements to follow a moving target (Royden et al. 1994; Warren and Hannon 1990). However, in this case, the optic flow is not the only information available to the subject because extraretinal signals such as a motor efference copy also are present. The need of such extraretinal signals for heading detection depends on speed, direction, and type or purpose of the eye movement (Banks et al. 1996; Royden et al. 1994; van den Berg 1993; Warren and Hannon 1990). For instance, very slow eye movements or eye movements that stabilize gaze on a stationary object in the environment do not necessitate an extraretinal signal for correct heading perception (van den Berg 1993; Warren and Hannon 1990). For studying optic flow processing, it is therefore crucial to know what eye movements occur during optic flow stimulation.

During the visual scanning of a radial optic flow stimulus, the visual motion pattern arriving on the retina depends on

0022-3077/98 $5.00

the direction of gaze. For instance, if the animal looks directly at the focus of expansion, the visual motion pattern is symmetric, and there will be no motion in the direction of gaze, i.e. on the fovea. If the animal looks in a different direction, retinal slip on the fovea will occur, the direction and speed of which will depend on the gaze direction. Therefore, the eye movement behavior is expected to also depend on the direction of gaze. Thus it is important to analyze the distribution of gaze directions and to link the analysis of the eye movement behavior to it. Moreover, this dependence of stimulus motion on gaze direction in principle demands a rapid adjustment of eye velocity after each saccade to a new position. Due to the latency of signals in the visual system such an adjustment cannot be done instantly. Therefore it is important to also investigate the dynamical properties of eye movements immediately after a saccade.

Optic flow stimuli differ from typical smooth pursuit stimuli because they contain large field motion. They also differ from typical optokinetic stimuli because the movement is not unidirectional. One major subject of this paper therefore will regard the nature of the eye movements elicited by optic flow stimuli in comparison with smooth pursuit and optokinesis.

Smooth-pursuit eye movements are elicited when a small moving object is attended and tracked with the eyes. The main purpose is to stabilize the image of an object on the fovea to maintain fixation. Gain is usually high for low and moderate target speeds, but it depends on the visual background surrounding the object. For example, with stationary structured background, gain decreases slightly and the number of catch-up saccades, which are necessary to compensate for positional errors, increases (Keller and Kahn 1986; Mohrmann and Thier 1995). Latency of the onset of pursuit is ~100 ms after the onset of target motion (Lisberger and Westbrook 1985).

Optokinetic eye movements are elicited when a large-field stimulus moves unidirectionally. First a saccade is made against the direction of the moving stimulus. Then a slow eye movements stabilizes the visual image on the retina. When gaze direction becomes about centered, a fast oppositely directed saccade resets the eye back to an eccentric position. Thus a regular pattern of interchanging slow and fast eye movements is observed. The eccentric range of eye positions covered by this pattern is known as the optokinetic ''Schlagfeld'' (Jung and Mittermaier 1939). The gain of the slow phases of the optokinetic nystagmus (OKN) is high for slow and median stimulus velocities (Cohen et al. 1977). Transparent motion in different directions inhibits OKN in humans (Niemann et al. 1994). Two different components of OKN can be distinguished based on the time course of their onset (Cohen et al. 1977). The early OKN (eOKN) shows a rapid rise of eye velocity soon after the stimulus starts. The late, or delayed, OKN (dOKN) shows a gradual buildup of slow phase eye velocity that takes several seconds to reach its maximum level. But the onset of an optokinetic response can be very fast. In the ocular following paradigm, a large field stimulus is initially at rest and then suddenly starts moving. Latencies of the occurring ocular following eye movements can be as small as 50 ms (Miles et al. 1986) and are especially small in the immediate wake of a saccade (Kawano and Miles 1986). The optokinetic reflex is thought to support the vestibular-ocular reflexes in stabilizing gaze during self-motion. Miles and Busettini (1992) suggest that the two components of optokinetic nystagmus, early and delayed OKN, might be related to and complement the two kinds of vestibular-ocular reflexes, the translational and the rotational VOR, respectively.

Smooth-pursuit eye movements are generated in a cortico-pontine-cerebellar pathway. It involves cortical areas MT, MST, the lateral intraparietal area (LIP), and 7A (Bremmer et al. 1997; Dürsteler and Wurtz 1988; Komatsu and Wurtz 1988; Sakata et al. 1983), the frontal eye field (Gottlieb et al. 1994), the dorsolateral pontine nucleus (DLPN) (Suzuki and Keller 1984; Thier et al. 1988), and parts of the cerebellum (Lisberger and Fuchs 1978). The basic circuit of the delayed OKN is relayed through the pretectal nucleus of the optic tract (NOT) (Hoffmann 1988) and the nuclei of the accessory optic system (AOS) (Mustari and Fuchs 1989). The evolutionary old velocity storage component of the dOKN involves the nucleus prepositus hypoglossi (NPH) and the vestibular nucleus (VN), which receive input from the NOT and the AOS. It is developed in all mammals. A monocular naso-temporal asymmetry in the gain of the slow phases in lower animals is overcome by a binocular cortical input to NOT and AOS in higher mammals such as cats and monkeys (Hoffmann 1981). The early OKN is thought to share main inputs with the smooth pursuit system and receive input from cortical areas MT and MST (Hoffmann et al. 1992). The ultrashort latencies observed in the ocular following paradigm are paralleled by visual neuronal latencies in MST, NOT, and DLPN (Hoffmann and Distler 1989; Kawano et al. 1992, 1994, 1996).

An analysis of oculomotor responses to radial optic flow stimuli has not yet been performed. In principle, oculomotor behavior during optic flow stimulation has to address two problems. If the optimal analysis of an environmental feature is required, for instance to determine its potential use or danger to the animal, smooth pursuit eye movement might be necessary to grasp and track the object with the eye. On the other hand, accurate estimation of the focus of expansion, i.e., of the direction of heading, might be required to inhibit eye movements in order to minimize the distortion of the radial optic flow pattern that inevitably occurs with any eye movement. But optic flow also might trigger involuntary optokinetic responses, which try to stabilize gaze and minimize foveal and parafoveal visual motion. If this is the case, then the dependence of these eye movements on parameters of the optic flow can impose important constraints on optic flow analysis. Knowing the pattern of eye movements that are elicited, perhaps even involuntarily, by radial optic flow is therefore essential for studying the mechanisms of optic flow processing.

METHODS

Eye movement recordings were performed in three awake male rhesus monkeys (*Macaca mulatta,* age between 4 and 7 yr).

Preoperative treatment

The monkeys first were trained to fixate a red spot of light. During training, no eye position registration was performed. Therefore monkeys learned to release a lever whenever a slight dimming

of the spot occurred. For the calibration, monkeys had to be able to fixate a spot of light (0.8° diam) for some seconds to allow precise adjustment of offset and gain of the recording equipment at the beginning of each session.

Animal preparation

After prior treatment with atropine and cortisone (Voren) and sedation with ketamine hydrochloride, deep anesthesia was obtained by intravenous injection of pentobarbital sodium (10 mg/kg, Nembutal). Under sterile conditions, a head-holder and two scleral search-coils, one for each eye, were chronically implanted. The search coils were connected to a plug on top of the skull. Postoperative antibiotics (Sobelin) and analgesics (Phenylbutazon) were applied. All experiments were in accord with published guidelines on the use of animal research (European Communities Council Directive 86/609/ECC).

Behavioral paradigm and data acquisition

The experiments were performed some weeks after the implantation, when the monkeys got used to the fixation of the head. During an experimental session, the monkey was seated in a primate chair with its head fixed. Horizontal and vertical eye movements of one eye were registered by an Eye Position Meter 3020 (Skalar). Eye position was calibrated first by playing a sequence of fixation points at different positions and adjusting offset and gain. Eye position data were recorded by a CED 1401 Interface (Scientific Products) with a sampling rate of 500 Hz and stored on a 486 PC. The software for experiment control and data recording (NABEDA—Neural And Behavioral Data Acquisition) was developed by M. Pekel.

In the experimental trials, no specific eye movement behavior was enforced. Each trial lasted 15 or 20 s. At variable time intervals (mean 4 s), a drop of apple juice was given to maintain the interest of the monkey. Intervals between two successive trials extended $\geq$20 s. Additional breaks of several minutes were given frequently. For each animal, recordings were performed on several days. Monkeys weight was monitored daily and supplementary fruit and water supply was provided.

On a single recording day, between 20 and 100 trials were performed. These contained different stimulus conditions that were randomly interleaved. With one exception, between 5 and 12 trials were collected per animal and stimulus condition. The exception was the recording of optokinetic responses in *monkey R*, where only one trial per stimulus direction and stimulus speed was performed. As described below, our data analysis is based on individual intersaccadic intervals of ~400 ms. Each recording trial contained between 37 and 50 of these measurements.

Visual stimuli

Optic flow stimuli were generated by a graphics work station (Silicon Graphics Indigo 2). The stimuli consisted of full-field computer-generated sequences that were back projected via a video projector onto a tangent screen, 47 cm in front of the monkey. The size of the stimuli covered a visual field of 90 × 90°. Optic flow sequences were generated on-line in real time with a frame rate of 60 Hz. We simulated egomotion of a virtual observer over a black extended horizontal plane, covered with white dots and located a certain distance h below eye-level (Fig. 1). We refer to this stimulus as the ground plane. The distance *h* corresponds to the eye-height of the observer. This stimulus was used for several reasons. First, we wanted a stimulus that simulated realistic optic flow as could be experienced readily during real self-motion. Yet we wanted it to be simple enough to allow a comparison between the stimulus and the eye movements. Second, it was necessary to use a stimulus in which a continuous constant flow field could be presented over an extended time. Third, the stimulus needed to consist of a smooth flow field in which each gaze direction could be associated with a unique visual motion. This association should not change over time. Fourth, using a ground plane allowed comparisons with findings from human psychophysical studies, which often used this kind of stimulus. The ground plane was truncated at a simulated distance of 36 eye heights in depth. As a result, the visible horizon was 1.6° below the horizontal median of the screen. As dots left the screen, new dots appeared along the horizon during the simulation periods. Approximately 250 dots were visible at each time. The dot size was kept constant (0.5°) during a trial. Luminance contrast was >99%.

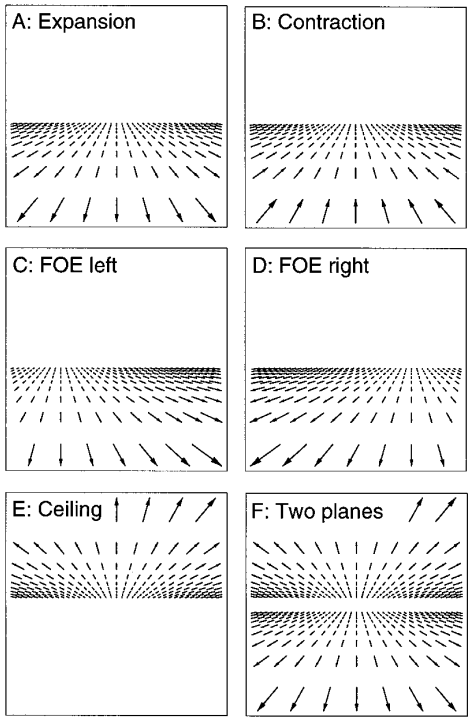

FIG. 1. Illustration of the optic flow stimuli. These stimuli simulated the movement of an observer with respect to a virtual visual environment. The environment consisted of a horizontal plane located a certain distance below eye level end extending 36 eye heights in depth. We refer to this as the ground plane. The plane was covered with lit dots, which moved on the screen according to the simulated observer motion. Forward motion resulted in expansion stimuli (*A*), backward observer motion resulted in contraction stimuli (*B*). Different directions of observer motion resulted in different positions of the focus of expansion on the screen (*C* and *D*). In addition, different observer speeds were used, resulting in different speeds of the individual motion elements. In one set of experiments, we also used an inverted version of the ground plane (*E*) and a condition with 2 planes, one below the observer and one above the observer (*F*).

Several parameters of the stimuli were independently varied in successive trials. First, the simulated observer velocity could take different values. Speeds in the optic flow scale with the observer velocity and the inverse of the eye-height. We used speeds of 2.73, 5.45, and 8.18 eye-heights per second. For a rhesus monkey of 37 cm height, these values would correspond to 1, 2, and 3 m/s forward speed. For a human of 1.65 m height, they would correspond to 4, 8, and 12 m/s. Second, the horizontal position of the focus of expansion was either in the center of the screen or was shifted 10 or 20° horizontally, thereby simulating observer movement in different directions (−20, −10, 0, +10, and +20°). Third, either forward or backward movement was simulated, resulting in an expanding or contracting flow field. In addition, some control ex-

periments were performed in which stimuli consisted of a virtual plane above the monkey or of two planes. Also, we employed regular optokinetic stimuli in which full-field two-dimensional unidirectional motion was presented.

The optic flow stimuli contained different optical velocities at different points on the screen. Different observer velocities also resulted in different optical velocities. The optical velocities ranged from 0.2 to 157°/s in the 1-m/s condition, from 0.52 to 313°/s in the 2-m/s condition, and from 0.78 to 470°/s in the 3-m/s condition. However, because the distribution of gaze of the animals occupied only a portion of the screen (see RESULTS), the highest optical velocities occurring in the direction of gaze were much smaller. Within the range of 90% of all gaze directions, maximum optical velocities were 27, 37, and 52°/s for the three observer velocities (1, 2, and 3 m/s), respectively.

Data analysis

Recorded data were first filtered with a Gaussian filter of 2 ms width. Then eye positions were plotted, and eye velocity was calculated by differentiation of the eye position data. From these data, slow eye movements and saccades could be distinguished clearly. We separated slow and saccadic eye movements by a velocity level criterion that was always adjusted well above the noise level and the velocities during the slow phases. Most often a velocity level of 25°/s was used. The beginning of a saccade was determined as the last data point with a velocity below this level. To determine the end of the saccade, we searched for the first data point with a velocity below the criterion level. An additional criterion for the classification of a saccade was a minimum duration of 12 ms between the beginning and end times.

Slow phase eye movements were analyzed with respect to several parameters. Slow phase duration was calculated as the time between two successive saccades. Mean horizontal and vertical eye position of a slow phase were determined as the mean between respective values at the beginning and end of the eye movement. We also analyzed direction, speed, and amplitude of the eye movement. These parameters were calculated from the result of a linear regression over all eye position data from within a single slow phase. As the duration of a slow phase was typically ~400 ms (see RESULTS) the regression typically involved 200 sample points.

For eye speed, the linear regression gives only an approximate average because eye speed often changed gradually during a slow phase. We therefore based our evaluations on detailed point-to-point comparisons of single samples as described in the following section. We searched to determine the gain during slow phase eye movements. Its calculation necessarily differed from standard gain measures. It is not possible to use standard methods because of the nature of the optic flow stimuli and their difference to classical optokinetic or smooth pursuit stimuli. In the optic flow stimuli, the movement of individual dots is accelerating, and the direction of the flow field vectors is inhomogeneous across the visual field. We chose to define the gain with respect to the idealized optic flow velocity on the fovea. This velocity in principle can be determined from the eye position data. We used a simple visual environment that simulated translation over a ground plane. For each eye position, we therefore could calculate the optic flow motion that occurs at that position based on the knowledge of the simulated observer motion and the spatial location of the simulated ground plane. This allows us to assign to each gaze direction an optic flow vector that remains constant throughout the trial. However, we need to refer to this optic flow vector as an idealized motion because we do not know exactly whether at the time when the gaze is directed at some position, an actual moving dot is present at that position. Nevertheless, this method allows to associate a specific vector of foveal motion with each eye position. The procedure used to calculate the gain therefore consisted of five steps.

1) For each data sample point, we determined the direction of gaze, i.e., horizontal eye position x and vertical eye position y, in a coordinate system defined by the projection screen.

2) The optic flow velocity $\mathbf{f} = (f_x, f_y)$ at that visual direction was calculated from the parameters of the simulated observer motion and the visual environment used for the stimulation. To obtain the optic flow motion at position $\mathbf{p} = (x, y)$ on the screen, we need to project the motion of a corresponding point $\mathbf{R} = (X, Y, Z)$ in the simulated three-dimensional world onto the two-dimensional screen (Heeger and Jepson 1992; Longuet-Higgins and Prazdny 1980). Under perspective projection with a focal length of 47 cm point $\mathbf{R}$ is projected onto

$$\mathbf{p} = \begin{pmatrix} x \\ y \end{pmatrix} = 0.47 \begin{pmatrix} X/Z \\ Y/Z \end{pmatrix} \tag{1}$$

Next we need to determine the motion of $\mathbf{p}$ on the screen. It results from the motion of $\mathbf{R}$ in the simulated three-dimensional (3-D) space. This motion in turn results from the translational velocity $\mathbf{T} = (T_X, T_Y, T_Z)$ and the possible (eye)-rotation $\mathbf{\Omega} = (\Omega_X, \Omega_Y, \Omega_Z)$ of the observer. The 3-D motion $\mathbf{F}$ of point $\mathbf{R} = (X, Y, Z)^t$ is thus

$$\mathbf{F} = -\mathbf{T} - \mathbf{\Omega} \times \mathbf{R} \tag{2}$$

Because we assume pure translation, this becomes

$$\mathbf{F} = -\mathbf{T} \tag{3}$$

The motion of $\mathbf{p}$ on the screen is obtained from differentiating $\mathbf{p}$ with respect to time

$$\mathbf{f}(x, y) = \frac{\mathrm{d}\mathbf{p}}{\mathrm{d}t} = 0.47 \begin{bmatrix} (\dot{X}Z - X\dot{Z})/Z^2 \\ (\dot{Y}Z - Y\dot{Z})/Z^2 \end{bmatrix}$$

Inserting *Eqs. 1* and *2* we find

$$\mathbf{f}(x, y) = \frac{1}{Z} \begin{pmatrix} -0.47T_X + xT_Z \\ -0.47T_Y + yT_Z \end{pmatrix} \tag{4}$$

So far the calculations have not assumed a specific virtual environment. To calculate the optic flow for the ground plane stimulus (Fig. 1*A*), we need to express Z as a function of the gaze position $\mathbf{p} = (x, y)$. In our case, Z is a function of y only

$$Z(y) = -0.47 \frac{h}{y}$$

where h denotes the height of the observer from the plane (eye height). Therefore, the flow velocity at a given point on the screen is

$$\mathbf{f}(x, y) = \frac{y}{0.47h} \begin{pmatrix} 0.47T_X - xT_Z \\ 0.47T_Y - yT_Z \end{pmatrix} \tag{5}$$

3) The eye velocity $\mathbf{v} = (v_x, v_y)$ was computed from the recorded eye position data.

4) The instantaneous gain g for the single data point was calculated as the ratio between the component of the eye velocity in the direction of the optic flow vector and the speed of the optic flow vector

$$g = |\mathbf{v}|/|\mathbf{f}| \cos(\alpha)$$

where α is the angle between the eye movement direction and the optic flow direction.

5) The mean gain of the slow phase was determined by averaging over the instantaneous gain values of all data points within the slow phase ($N \approx 200$).

Because the preceding analysis needed to associate each eye position with a specific optic flow stimulation on the fovea, it required that the point of gaze had to be located on the virtual

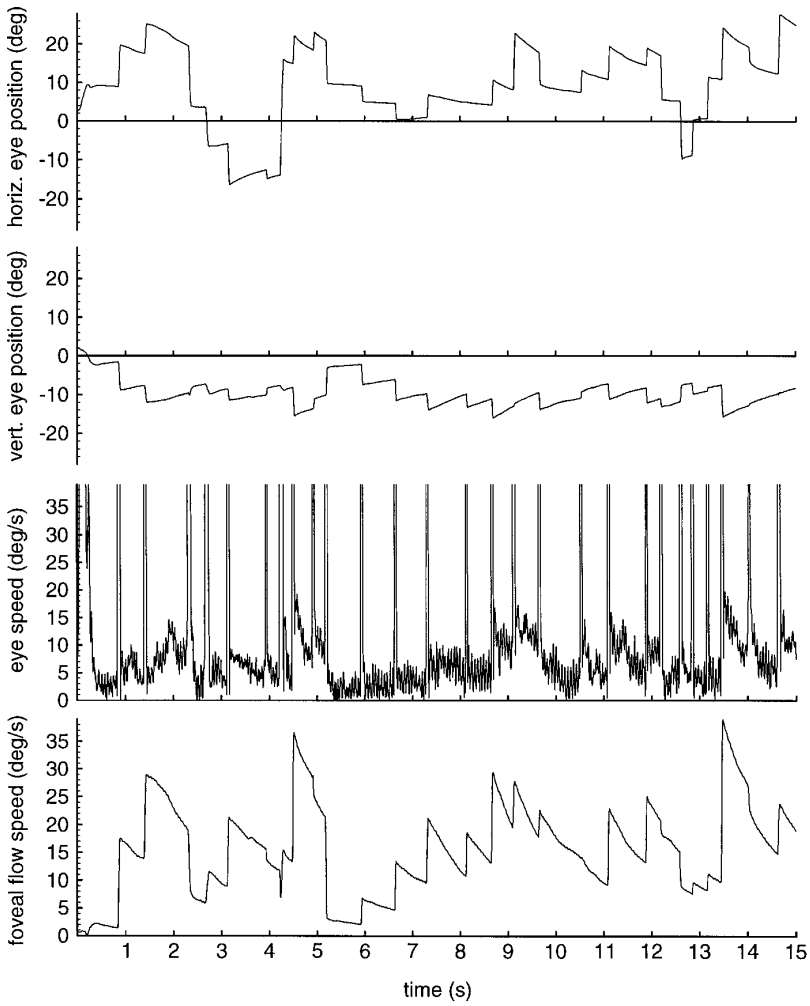

FIG. 2. Horizontal and vertical eye position and eye velocity traces as the monkey watched a contracting optic flow stimulus. Simulated observer speed was 3 m/s. Focus of expansion was in the center of the screen.

ground plane. Therefore, gaze positions occurring above the simulated horizon had to be excluded from the analysis and were discarded. However, this occurred only rarely, as >94% of all gaze directions fell on the simulated ground plane.

For most of the parameters we analyzed, the measured values did not follow a Gaussian distribution. We therefore evaluated the significance of the measurements in general by nonparametric statistical tests [*U* test, Kruskal-Wallis analysis of variance (ANOVA) on ranks with Dunn's test individual comparisons]. Consequently, we present medians rather than means in the graphs.

RESULTS

General properties of eye movements

Figure 2 shows a typical eye position and velocity trace during presentation of an optic flow stimulus. The velocity trace shows the absolute vectorial speed of the eye movement, i.e., the length of the eye movement vector. Also shown is a trace of the absolute optical speed in the direction of gaze, i.e., the magnitude of the foveal stimulus velocity, which was computed from the eye position data. The stimulus simulated backward movement (contraction) with a centered FOE. The monkey usually kept its eyes vertically within 15° of the visible horizon. The horizontal gaze direction varied over a wide range. One clearly can see slow eye movements directed toward the vertical meridian, suggesting that gaze roughly followed stimulus motion. The slow eye movements are disrupted by saccades at regular intervals. The velocity traces also show the two alternating phases clearly.

To illustrate the relation of the slow phase eye movements to the optic flow stimulus, we constructed vector field plots of the eye movement data. Figure 3*A* depicts such a plot for one monkey showing eye movements during simulated forward movement of 2 m/s. In this figure, vectors indicate starting position, direction, and speed of all single slow phase eye movements recorded with this stimulus in several trials. The eye movement speed was a result of a linear regression over unfiltered raw eye position data and represents a mean speed over the whole slow phase interval. To compare the pattern of eye movements with the pattern of the optic flow stimulus, we plotted idealized optic flow vectors arising at the recorded gaze positions (Fig. 3*B*). This figure shows the local speed and direction in the stimulus for every mean eye position of each slow phase from Fig. 3*A*. Figure 3 shows an excellent correspondence of eye movement direction and local motion direction on the fovea for most eye movements. However, one also can observe that the eye speed is often considerably lower than the corresponding local stimulus speed. In the following sections, we will quantify this behavior and also analyze the distribution of gaze directions during a trial.

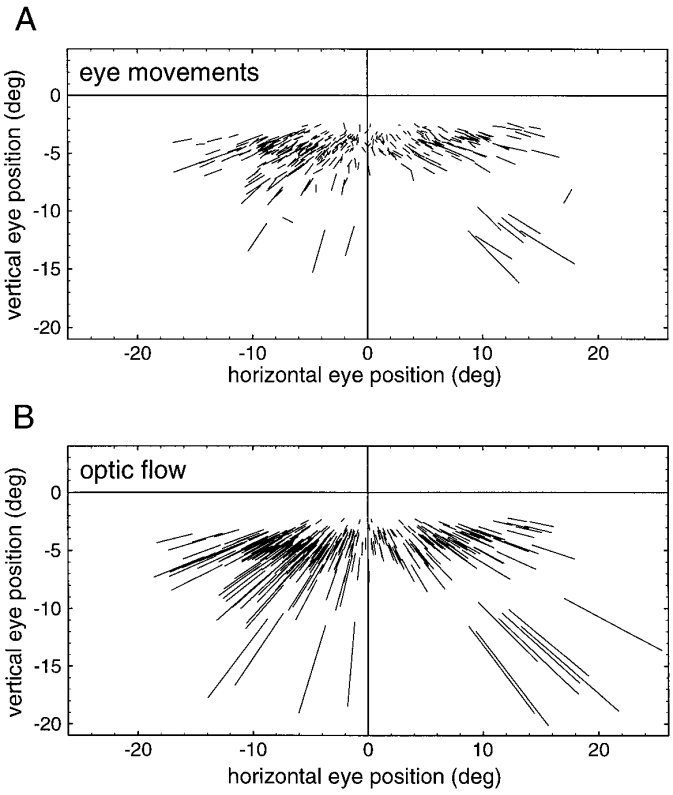

FIG. 3. Vector field plot of the eye movement data. *A*: slow phase eye movements during an expanding flow field with a simulated observer speed of 2 m/s. Each individual line indicates starting position, mean direction, and mean speed of a single slow phase eye movement, which on average lasted for 400 ms. *B*: optic flow vectors that occurred at the recorded eye positions in *A*. Each vector represents the local speed and direction in the stimulus at an eye position that corresponded to the mean eye position during one of the slow phases.

Distribution of gaze directions

For the analysis of gaze directions, a single average eye position was computed for each slow phase by taking the mean of the start and end positions. Examples of the distribution of horizontal and vertical eye positions for the three monkeys are shown in Fig. 4. These examples depict eye positions during a stimulus that simulated forward motion of 2 m/s with a centered FOE. The distribution of gaze is very similar for all three monkeys. Horizontal eye positions are centered around the straight ahead direction and stay within the central 40°. The histograms of vertical eye positions show a steep decrease for eye positions below −5°. It is evident that the eyes are not kept exactly at the horizon but rather a few degrees below.

Because the behavior of the three monkeys was very similar, we combined their data. Median eye position of the combined sample was at −2.16° horizontally and −4.15° vertically. These values change little with observer speed. The same was true for the horizontal range of eye positions. However, the vertical range of eye positions decreased when the simulated observer speed increased. We also found that median vertical eye position was similar for expansion and contraction stimuli and was independent of the position of the FOE.

For horizontal eye position, we were interested especially in the question of whether eye position shifts with the horizontal position of the focus of expansion. Because the FOE is an important feature of the flow field and its position relative to the direction of gaze strongly influences the retinal motion input to eye movement generation systems, an orientation of gaze toward the FOE might be expected. We found that median horizontal eye position indeed significantly varies with the position of the FOE in expansion stimuli (Fig. 5*A*, Kruskal-Wallis ANOVA, $P < 0.01$). However, the magnitude of the shift of eye position was much smaller than the shift of the FOE position. For contraction stimuli, we observed an adverse behavior: the median horizontal eye position shifts in the opposite direction from the focus of contraction (Fig. 5*B*). This shift is also highly significant (Kruskal-Wallis ANOVA, $P < 0.01$). Thus it appears that gaze position is not influenced by the position of the singular point alone but rather by a combination of the position of the singular point and the directions of visual motion.

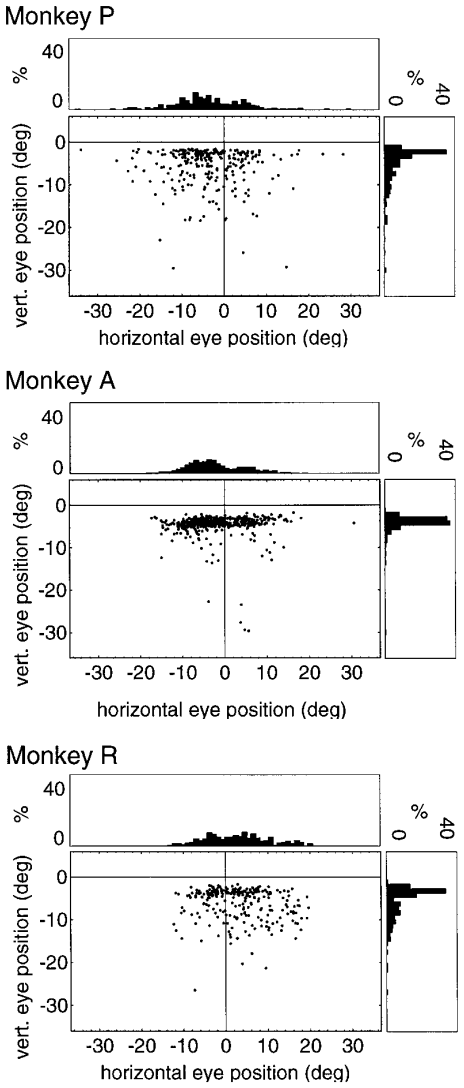

FIG. 4. Distributions of horizontal and vertical gaze positions obtained with a centered FOE and 2 m/s simulated observer speed for 3 monkeys. Each dot refers to the mean eye position during one slow phase. *Top* and *right*: frequency distribution histograms of horizontal (*top*) and vertical (*right*) eye positions.

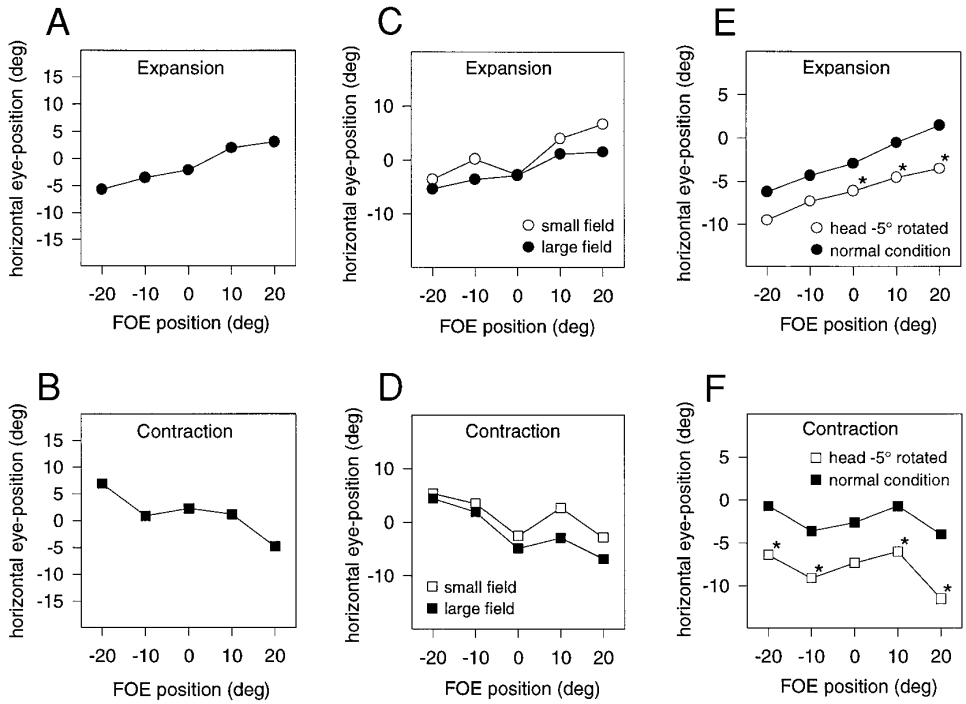

FIG. 5. Dependence of the median horizontal eye position on the location of the focus of expansion, stimulus extent, and the direction of the naso-occipital axis of the monkey. *A* and *B*: median horizontal eye positions during large-field expansional (*A*) and contractional (*B*) optic flow depend on location of the focus of expansion (FOE) [$P < 0.01$, Kruskal-Wallis analysis of variance (ANOVA)]. Data were pooled across all 3 monkeys; each point is the median of ~900 slow phases in the case of expansion and ~700 slow phases in the case of contraction. *C* and *D*: influence of stimulus borders on median horizontal eye position for one monkey. A smaller stimulus ($50 \times 50°$) with centered FOE was used. Placing it at different points on the screen varied the position of the stimulus borders along with the FOE position. ○ and □, median horizontal eye positions for these stimuli across all slow phases ($n = 60 \cdots 215$). ●, and ■, median eye positions with the large stimuli of this monkey for comparison ($n = 400 \cdots 491$). *E* and *F*: influence of head position on median horizontal eye position. In one monkey, the head was manually turned and adjusted 5° to the left. ○ and □, median horizontal eye positions in this condition ($n = 62 \cdots 169$). ■ and ●, median horizontal eye positions for a centered head position in this monkey ($n = 169 \cdots 310$). Large stimuli were used for both head positions. * Significant differences between the head-straight and the head-turned condition (*U* test, $P < 0.05$).

There are at least two more parameters that potentially could influence horizontal eye position. First, horizontal eye position might shift with a positional change of the horizontal borders of the stimulus rather than with the position of the FOE. This assumes that the preferred gaze direction of the monkeys may be associated with the symmetric extent of the visual stimulus. A second possibility is a preferential alignment of the median gaze direction with head direction. To test the first hypothesis, we used a smaller stimulus of $50 \times 50°$ size. We now varied not only the position of the focus of expansion but also the position of the borders along with it. In this way, the stimulus was always symmetric around the FOE. This experiment was performed in one monkey only. We found that the variation of the median horizontal eye position was very similar with the full-field and the small-field stimulation (Fig. 5, *C* and *D*). Thus the border placement and the symmetry of the stimulus did not appear to affected the horizontal eye position.

In one monkey, we tested the effect of a change in head direction from 0° (naso-occipital axis points to the center of the screen) to −5° (naso-occipital axis is turned 5° to the left). The results are shown in Fig. 5, *E* and *F*. Comparing the median eye positions in the two situations, for all FOE positions, we found a shift to the left when the naso-occipital axis was turned to the left. This shift ranged from −3.8 to −5.7°, indicating that the head direction is a critical parameter that influences the distribution of gaze directions. Monkeys tended to keep their horizontal gaze direction mainly aligned with the naso-occipital axis. In summary, we found opposite influences of the position of the FOE on the horizontal eye position in expansion and contractions stimuli, and a strong influence of the head position.

Direction of slow phase eye movements

In an optic flow stimulus, local motion direction depends on position within the stimulus. Likewise the direction of slow phase eye movements depended on eye position in a predictable manner. We wanted to quantify the relationship between the eye movement and the local optic flow motion on the fovea. We computed the angular difference between the average eye movement direction during a slow phase and the direction of the optic flow vector on the fovea. In general, we found a good correspondence of the foveal flow direction and the eye movement direction for all types of flow stimuli. Figure 6 shows distribution histograms for two particular stimuli. In Fig. 6*A*, the stimulus consisted of an expansion with the FOE centered on the screen. The majority

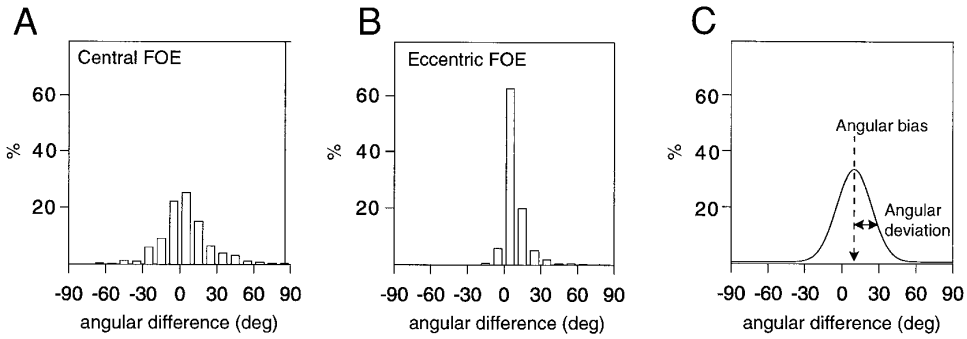

FIG. 6. Two examples for distributions of angular differences between the eye movement direction and the direction of the optic flow at the gaze position. Mean angular difference for each slow phase was obtained by comparing the mean direction of the eye movement with the direction of the motion on the fovea. Direction of motion on the fovea was computed from the parameters of the stimulus and from the gaze positions during the slow phase. *A*: distribution of angular differences for an expansion stimulus with centered FOE. Simulated observer speed was 2 m/s. *B*: distribution of angular differences for an expansion stimulus with the FOE located 20° eccentric on the screen. Simulated observer speed again was 2 m/s. *C*: illustration of the definitions of angular deviation and angular bias. Angular deviation is defined as the spread of the angular differences, given by the half-width of the distribution. It is computed as the difference of the 1st and 3rd quartile divided by 2. Angular bias is defined as the average offset between the direction of the eye movement and the direction of the stimulus motion on the fovea, i.e., as the median of the distribution of angular differences.

of all angular differences is $<20°$ with the center of the distribution at 0°. The distribution is even narrower in Fig. 6*B*, where the FOE is placed 20° eccentric on the screen. But for eccentric FOE positions, the center of the distribution is shifted away from zero, i.e., a systematical directional error (angular bias) occurs. We quantified both the average magnitude of the angular deviation, i.e., the spread of the eye movement direction with respect to the direction of the foveal motion, and the angular bias, i.e., the average offset of the eye movement direction from the foveal motion direction (Fig. 6*C*).

A quantitative measure of the average angular deviation of the directional following is the half-width of the distribution of angular differences (Fig. 6*C*). To determine this, we took the difference between the upper and lower quartiles of the distribution and divided by two. Figure 7*A* shows the angular deviations for centered FOE and different observer speeds. In this situation, contracting flow fields yielded a smaller angular deviation than expanding stimuli. With increasing observer speed (resulting in increasing stimulus speed), the angular deviation decreased. Also, for increasing observer speed, the differences between expanding and contracting stimuli decreased. The angular deviation also depended on the placement of the focus of expansion (Fig. 7*B*). When the horizontal FOE position became more eccentric, angular deviation decreased both for expanding and contracting flow fields.

To quantify the angular bias, we determined the median value of the angular differences. Counter-clockwise deviations from the foveal stimulus direction were counted positive, clockwise deviations were counted negative. Figure 8*A* shows that FOE position leads to systematic changes in the angular bias, both for expansion and for contraction (Kruskal-Wallis ANOVA, $P < 0.01$). For rightward FOE positions, the angular bias is positive (clockwise), whereas for leftward FOE positions, the angular bias is negative (counterclockwise). Figure 8*B* schematically illustrates the angular bias for expansion and contraction. For expansion, the eye movement direction is rotated downward for both positive and negative focus positions. For contraction, eye movement direction is in both cases rotated upward. This effect suggests an influence of the global motion direction because it is in the direction of the global resultant stimulus

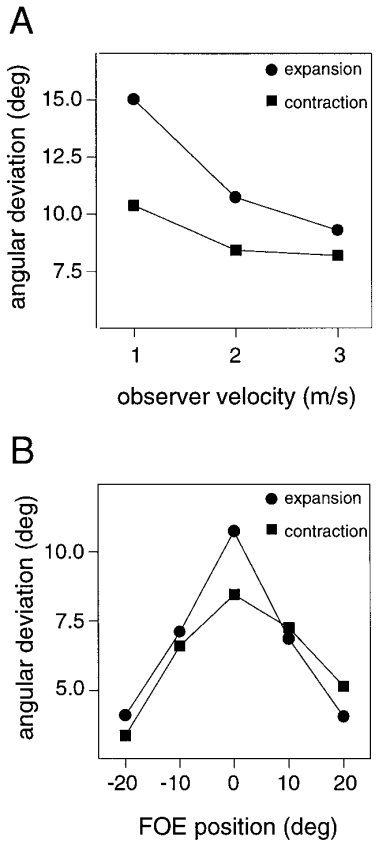

FIG. 7. Dependence of the angular deviation on observer velocity (*A*) and FOE position (*B*). Angular deviation was defined as half the difference between the upper and lower quartile of the distribution of angular differences (Fig. 6*C*). For *B*, only stimuli with observer velocity of 2 m/s were used.

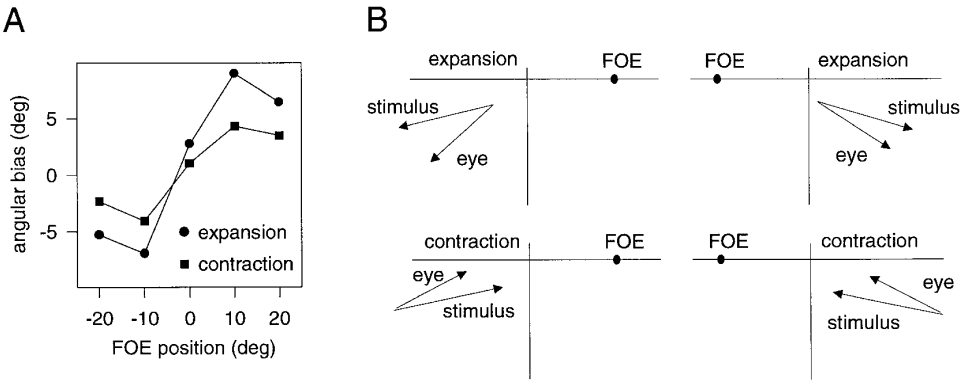

FIG. 8. Angular bias of slow phase eye movement direction. Angular bias is defined as the median of angular differences between eye movement direction and foveal flow direction (Fig. 6*C*). *A*: angular bias depends on horizontal FOE position for both expansion and contraction (Kruskal-Wallis ANOVA, $P < 0.01$). *B*: schematic illustration of the results. For expanding stimuli, the eye movement direction is tilted downward from the local flow field direction. Contracting stimuli lead to the opposite effect. Both situations suggest influences of the global motion pattern on the foveal following because the angular bias is always in the direction of the global resultant motion of the stimulus. Each point is the median of ~900 measurements in the case of expansion and ~700 measurements in the case of contraction.

motion, which is downward for expansion and upward for contraction.

Velocity and gain of slow phase eye movements

For increasing observer speed, and hence for increasing flow field speeds, the median eye movement speed also increased linearly both for expansion and contraction. Median eye speed ranged from 0.74°/s (expansion, 1-m/s observer speed, central FOE) to 6.2°/s (contraction, 3-m/s observer speed, FOE 20° eccentric). As with the angular deviation, we defined the gain of a slow phase eye movement with respect to the local flow velocity on the fovea, computed from the eye position data and the stimulus parameters and averaged across all sample points (typically ~200) during a slow phase (see METHODS). With this measure, we found the gain to be considerably smaller than one. Figure 9*A* displays a histogram of the distribution of gain values. The distribution peaks near a value of 0.5. The broad shape of the distribution suggests that the speed of slow phase eye movements is only weakly linked to the speed of the foveal motion.

Figure 9*B* shows that the median gain is unaffected when observer velocity and therefore flow field speed changes. However, we observed a consistent difference in gain between expansion and contraction. For expansion, the median gain values (0.40–0.45) were always significantly lower than for contraction (0.57–0.60) (*U* test, $P < 0.05$). Figure 9*C* shows the variation of the median gain with the position of the FOE. For expansion, the gain revealed a significant modulation (Kruskal-Wallis ANOVA, $P < 0.01$). Median gain is lowest for central FOE position and increases when the FOE becomes more eccentric. For contraction, we also found a significant modulation (Kruskal-Wallis ANOVA, $P < 0.01$), but median gain increased significantly only for leftward eccentric FOE positions.

In the ground plane condition, expansion stimuli always have a mean resultant downward motion. Mean resultant motion of contraction stimuli is always directed upward. In monkeys and man, optokinetic responses are different for upward and downward motion (Matsuo and Cohen 1984; Murusagi and Howard 1989; van den Berg and Collewijn 1988). Upward motion leads to stronger OKN and higher gain than downward motion. We wanted to see whether such an asymmetry is reflected in the oculomotor behavior in our condition and whether it could account for the gain differ-

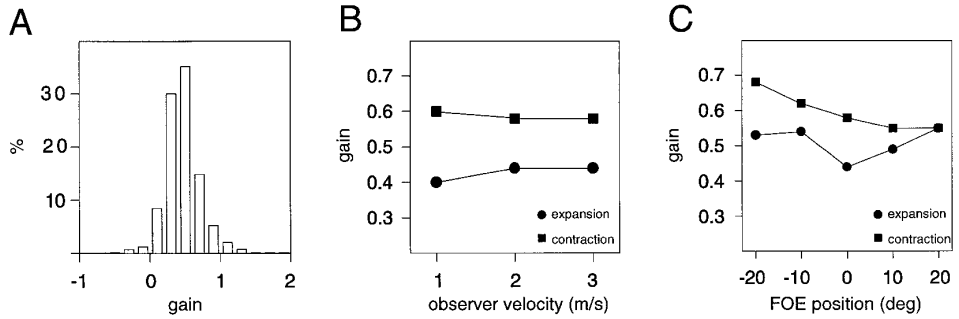

FIG. 9. Gain of the slow phase eye movements. Gain for each slow phase was defined as the ratio between the eye speed in the direction of the foveal motion and the speed of the foveal motion, averaged over all data points within the slow phase. *A*: distribution of gain values for central FOE and 2 m/s simulated forward observer motion. *B*: medians of the gain for different observer velocities and central FOE. Difference between expansion and contraction is highly significant (*U* test, $P < 0.01$; $n = 983{,}971{,}742$ for expansion, 716,735,528 for contraction). *C*: medians of the gain (2 m/s observer speed) depended on FOE positions (Kruskal-Wallis ANOVA, $P < 0.01$, $n \approx 900$ for expansion, 700 for contraction).

ences between expansion and contraction. Therefore, we analyzed the gain in relation to the direction of the eye movement. To do this, gain values from individual slow phases were sorted by the average direction of the eye movement during the slow phase. Median of the gain then was determined across those slow phases that shared a similar direction. Data from all stimulus types were included. For comparison, we also measured the gain to regular OKN stimulation in different directions. For this, full-field unidirectional motion of random dot patterns was presented. About the same number of dots as in the ground plane conditions were used. In subsequent trials, five different visual speeds (2.5, 5, 10, 20, and 30°/s) were used and the recorded data was pooled to result in a comparable distribution of speeds as in the optic flow stimuli. Figure 10 displays the median OKN gain and the median optic flow gain separately for the two monkeys tested. A Kruskal-Wallis ANOVA revealed significant variations of the gain with the direction of the eye movement for both OKN and optic flow in both monkeys. Individual comparisons of OKN gain and optic flow gain for individual directions revealed significant differences between the two stimulus conditions for all directions in *monkey A* and for up and down directions in *monkey R* (Dunn's test, $P < 0.05$). Clearly there is a strong horizontal-vertical asymmetry of the OKN in *monkey A.* The gain is distinctly higher for horizontal than for vertical eye movements. Also a small up-down asymmetry can be observed. The second monkey showed no horizontal-vertical asymmetry but a stronger up-down asymmetry. Very similar directional variations of the gain are observed during optic flow stimulation, although the absolute gain values are much lower in that case.

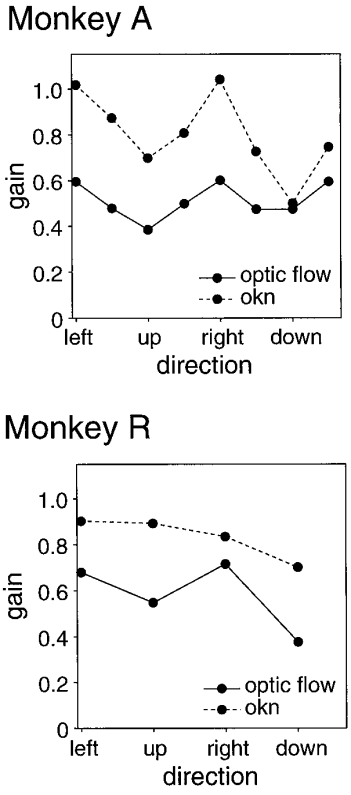

FIG. 10. Comparison of the gain during optic flow stimulation with the gain during pure optokinetic stimulation for different eye movement directions. Data from 2 monkeys are shown separately. For OKN stimulation, a full field unidirectional motion of dots was used. In both monkeys, the modulations of optic flow gain and OKN gain were significant (Kruskal-Wallis ANOVA, $P < 0.01$). For all directions in *monkey A* and for the up and down directions in *monkey R,* the differences between OKN and optic flow were also significant (Dunn's test, $P < 0.05$). Data were combined from all optic flow stimuli for the optic flow condition, and for different speeds (2.5–30°/s) in the OKN condition ($n = 379 \cdots 571$ for OKN and $444 \cdots 2{,}111$ for optic flow in *monkey A;* $n = 27 \cdots 173$ for OKN and $366 \cdots 648$ for optic flow in *monkey R*).

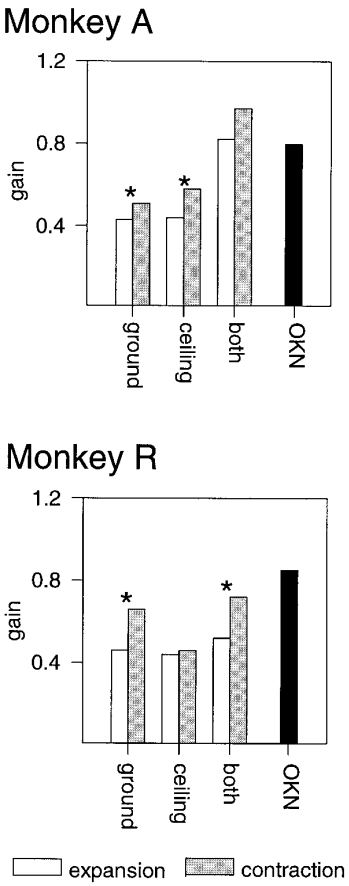

FIG. 11. Median gain values of 2 monkeys for 4 different stimulus types. First stimulus was the ground plane flow field (Fig. 1*A*). For the 2nd stimulus type, the ground plane flow field was presented upside down as if the observer moved below a ceiling. Third stimulus consisted of 2 planes, one below and one above the observer. Fourth stimulus (OKN) displayed full field unidirectional motion. Significant differences (*U* test, $P < 0.01$) between expansion and contraction are marked (*, $n = 192 \cdots 3{,}743$ for *monkey A;* $n = 195 \cdots 769$ for *monkey R*).

To test whether the gain difference between expansion and contraction is related to the up-down asymmetry of OKN, we disassociated expansion/contraction from upward/downward motion. We therefore presented an inverted stimulus that simulated movement below a ceiling. In this stimulus, expansion results in upward motion and contraction results in downward motion. We also presented a full-field stimulus consisting of two planes of dots, one below the observer (the ground plane) and one above the observer (the ceiling plane). In this stimulus, resultant global motion is zero. Figure 11 shows the median gains for these three conditions. In all cases, the gain is lower for expansion than for contrac-

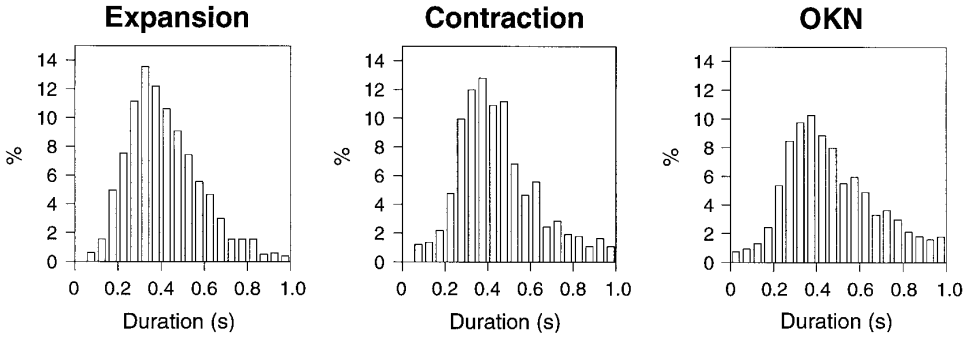

FIG. 12. Frequency histograms of the distributions of slow phase durations for expansion, contraction, and regular optokinetic stimulation.

tion. In one monkey, the gain increased significantly when the full-field stimulus was presented rather than the half-field stimuli (U test, $P < 0.05$). These results show that the optokinetic up-down asymmetry cannot explain the gain difference between expansion and contraction.

Duration of slow phase eye movements

We observed a quite regular interchange of slow and fast eye movement phases. Figure 12 shows distributions of the durations of slow phases for expansion and contraction stimuli. For comparison, Fig. 12 also shows the distribution of slow phase durations during full-field optokinetic stimulation. The distributions in all three cases are very similar. Typical durations of slow phases ranged from 200 to 600 ms. Medians were 405 ms for expansion, 425 ms for contraction, and 470 ms for OKN. The differences were therefore small but significant (U test, $P < 0.05$). Duration of slow phases was unaffected by observer velocity or placement of the FOE. The single peak and the restricted range of the slow phase durations in all conditions demonstrate the regularity of the interchange between slow and fast phases.

Catch-up saccades

One parameter that could help identify the possible involvement of the smooth pursuit eye movement system is the relation of saccadic amplitudes and directions to the direction of the preceding slow phase eye movement. Typically during smooth pursuit, when the speed of the eye does not match the speed of the target and thus the distance of the target from the fovea increases, a saccade is initiated to bring the target back on the fovea. Such catch-up saccades are typically small in amplitude and directed along the direction of the smooth eye movement. Fast eye movements of the optokinetic system, on the other hand, are used to compensate the positional drift during slow phase eye movements and are therefore in the opposite direction from the preceding slow phase eye movement. Therefore, if the smooth pursuit system is involved in the case of our experiments, a high occurrence of catch-up saccades would be expected because of the low gain generally observed.

We calculated for each saccade its amplitude and the difference of its direction to the direction of the previous slow eye movement. We then looked for the number of saccades that had amplitudes $<1°$ and direction that deviated from the direction of the previous eye movement by $<20°$. Based on these criteria, $<1\%$ of all saccades qualified as potential catch-up saccades. Therefore we conclude that nearly all saccades are directed to new visual targets or new gaze positions.

Dynamical properties

Dynamical properties of slow phase eye movements were analyzed on two different scales. The first involved an analysis of the gain over the length of the stimulation (20 s). Second, the development of the gain and of the directional following was analyzed during the course of a single slow phase. Finally, we also looked at cross-saccadic effects, i.e., influences on gain and angular deviation from the preceding slow phase.

The optokinetic nystagmus can be divided into the early and the late OKN. Characteristic of the late OKN is a slow buildup of the gain during the first few seconds of stimulation. When the stimulus is suddenly switched of and the animal is in darkness, the nystagmic eye movements continue with a slow decay over several seconds (optokinetic after-nystagmus). We calculated medians of gain values at 2-s intervals. The gain did not change during the 20-s presentation time. In occasional observations, we found only weak indications for the presence of an optokinetic after-nystagmus following optic flow stimulation. However, one has to keep in mind that the gradual buildup as well as the gradual decay of the delayed OKN are attributed to the loading and unloading of a neural integrator. The constant change of eye movement direction in consecutive slow phases might prevent a loading of this integrator. Therefore, the conditions under which the temporal buildup or the after-nystagmus can be observed might not be met in this case.

We next looked at the temporal development of the gain during individual slow phases. Of special interest in this regard is the initial part of the slow phase, immediately after the saccade, when visual feedback is not yet available. Because the visual motion at the new gaze direction is different from the visual motion during the preceding slow phase, it is important to determine how the eye adapts to this new situation. To calculate the time course of the gain, a time window of 20 ms was moved in 10-ms steps over the eye position data. Within this time window, the average gain was determined by calculating the gain for each individual sample point ($n = 10$) and averaging across the resulting individual gain values. Then the median gain was calculated across all slow phases ($n > 693$). Such median gain values at 10-ms time intervals were evaluated separately for slow phase eye movements in two different conditions. The first

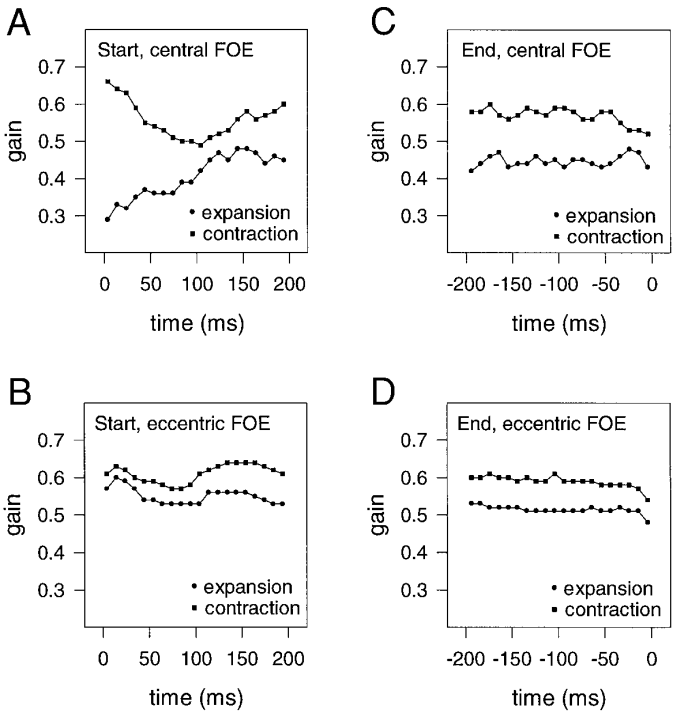

FIG. 13. Temporal development of the gain during a slow phase. Median gain for 20-ms bins was calculated every 10 ms. Gain values from all slow phases were pooled, and the median was determined. *A* and *B*: median gain within the 1st 200 ms of each slow phase for central (*A*) or eccentric (*B*) FOE position. All slow phases were aligned to the end of the preceding saccade. *C* and *D*: median gain during the last 200 ms of the slow phase for central (*C*) or eccentric (*D*) FOE position. Here, slow phases were aligned to the start of the terminating saccade. Gain is constant until the end of the slow phase. Stimuli were movements of 2 m/s over a ground plane. For the eccentric FOE position in *B* and *D*, data from trials with −20 and +20° eccentricity were pooled. Each point is the median of 883 and 1,712 measurements for expansion with central or eccentric FOE and 693 and 1,244 measurements for contraction, respectively.

condition comprised flow fields with a central FOE position. The other consisted of flow fields with a focus position at −20 or +20°. All three virtual observer velocities were included, but a minimum duration of 250 ms for any single slow phase was required.

Figure 13, *A* and *B*, shows the development of the gain within the first 200 ms of the slow phases. Figure 13, *C* and *D*, presents the gain within the final 200 ms of slow phases for comparison. In Fig. 13, *C* and *D*, slow phases were aligned with respect to the onset of the terminating saccade. At the end of the slow phases, the gain is constant but different for expansion and contraction. In the initial part, however, different time courses are observed for expansion and contraction in the central FOE condition (Fig. 13*A*). The gain is initially low for expansion and increases within the first 120 ms to a steady state value >0.45. For contraction, an opposing effect is observed: the gain is initially high and decreases within the first 100 ms to 0.5 after which it increases again. These effects are not observed when the focus position is eccentric (Fig. 13*B*). In all cases, the gain values for expansion were below those for contraction.

For centered FOE stimuli, we also analyzed the development of the angular deviation during the initial part of the slow phase (Fig. 14). The procedure was equivalent to the analysis of the temporal development of the gain. Angular differences were calculated in 10-ms steps during each slow phase. Then the angular deviation was determined across all slow phases ($n > 693$). This resulted in a picture of the time course of the angular deviation during an average slow phase. For expansion, the angular deviation initially after a saccade was remarkably high but decreased within the first 100 ms after the saccade to the low value we observed previously. For contraction, the results were quite different. There the angular deviation was low already immediately after the saccade and throughout the slow phase.

The angular deviation during expansion was initially very large. We wondered whether this might be related to the ongoing eye movement before the saccade, i.e., during the preceding slow phase. We therefore asked whether the initial angular deviation depended on the directional difference between the preceding slow phase and the current foveal motion stimulus. We sorted slow phases according to the difference between their initial foveal stimulus direction and the direction of the eye movement that was performed during the slow phase preceding to the saccade. We then calculated the median of the initial angular deviation for four different directional difference classes, 0–45, 45–90, 90–135, and 135–180°. We used only the first 40 ms of each slow phase for the calculation of the initial angular deviation and the initial foveal stimulus direction. Figure 15*A* shows the result. For expansion, the initial angular deviation is low when the new stimulus direction is similar to the direction of the preceding slow phase eye movement and is much higher when the directional difference is larger. In contrast, initial angular deviations are always much lower for contraction. We also analyzed the dependence of the median gain in the initial 40 ms after a saccade on the difference between the initial foveal stimulus direction and the direction of the eye movement during the previous slow phase (Fig. 15*B*). For contraction, the initial gain was uniformly high regardless of the directional difference between the current stimulus and the previous eye movement. For expansion on the other hand, the gain strongly decreased as the angular difference between the current stimulus direction and the direction of the previous slow phase increased. When this angular differ-

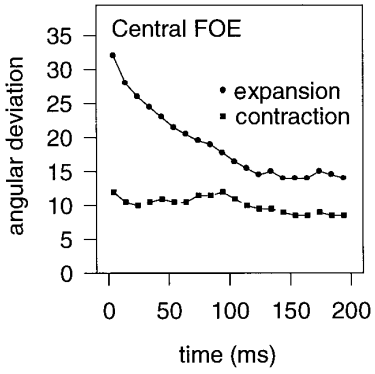

FIG. 14. Temporal development of the angular deviation during the initial part of a slow phase, i.e., immediately after the saccade. Data are from movements at 2 m/s over a ground plane with a central FOE position. Angular differences between eye movement direction and foveal flow directions was calculated every 10 ms. Angular deviation at 10-ms intervals was determined from the distribution of angular differences across all slow phases ($n = 883$ for expansion and 693 for contraction) at that time interval.

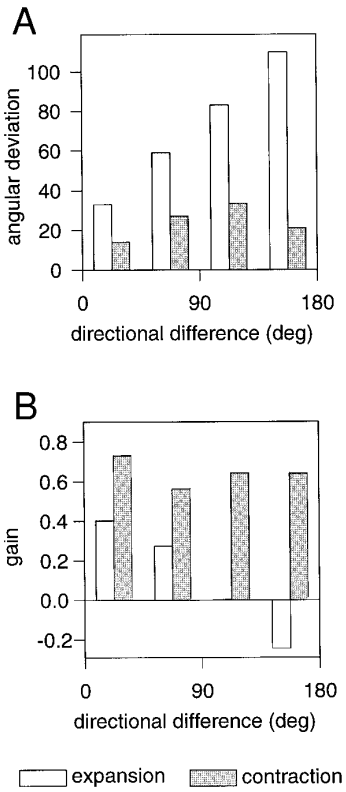

FIG. 15. Dependence of the initial angular deviation (*A*) and the initial gain (*B*) on the direction of the preceding slow phase. Horizontal axis indicates the angle between the direction of the foveal motion for any given slow phase and the direction of the eye movement during the preceding slow phase. Based on this angle, slow phases have been distributed into 4 bins, 45° wide (horizontal axis). Vertical axis gives the median angular deviation (*A*) and gain (*B*) during the initial 40 ms after a saccade (n = 1,241, 512, 518, and 144 for expansion; 1,065, 301, 248, and 78 for contraction).

ence was >135°, the median of the initial gain even reached negative values, i.e., eye movement was opposite to stimulus movement. This is in accordance with the observation that the median initial angular deviation was >90° in this condition.

This behavior clearly reveals a cross-saccadic influence on the angular deviation in the initial part of the slow phase. This led to the question whether and to what extent the initial eye movement direction is biased toward the direction of the preceding slow phase. To analyze this, we defined an index for each slow phase that measured how much the eye movement direction after a saccade deviated away from the foveal stimulus direction and into the direction of the preceding eye movement. This ''previous-direction influence'' (PDI) index was calculated as the angular difference between the current eye movement direction and the current foveal stimulus direction relative to the angular difference between the direction of the preceding eye movement and the current foveal stimulus direction [PDI index = (current eye movement − current foveal flow)/(previous eye movement − current foveal flow), see Fig. 16*B*]. The PDI index is 0 when the current eye movement is in the direction of the foveal flow and 1 when the current eye movement is in the direction of the previous eye movement. Figure 16*A* shows the distribution of the PDI index for expansion and contraction (centered FOE). When the full slow phase is considered, the distribution of the PDI indices is centered around 0 (median: 0.04 for expansion, 0.03 for contraction). This again shows that on average during the full slow phase the eye movement direction is aligned with the foveal stimulus. However, when only the initial 40 ms of the slow phase is analyzed, the distribution in the case of expansion is strongly shifted toward higher values of the PDI index, i.e., in the direction of the previous eye movement (median: 0.65). This is not the case for contraction (median: −0.01).

These results show that for expansion most deviations of the initial eye movement direction from the stimulus direction are indeed toward the direction of the preceding slow phase. However, while the initial eye movement direction deviates from the local flow field direction, it also deviates from the direction of the preceding slow phase. The initial eye movement direction after a saccade thus represents a

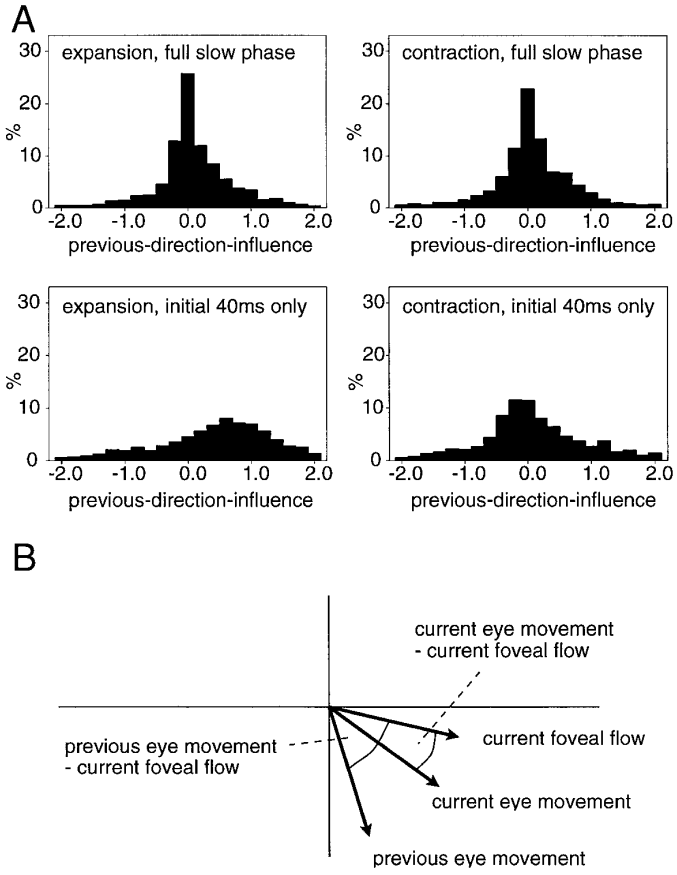

FIG. 16. Relationship of the initial angular deviation with the direction of the preceding slow phase and the current stimulus direction. We defined a ''previous-direction influence'' index (PDI index), which measured the alignment of the eye movement with the current foveal stimulus and with the direction of the eye movement during the previous slow phase, i.e., before the saccade to the new gaze position [PDI index = (current eye movement − current foveal flow)/(previous eye movement − current foveal flow)]. This index is 0 when the current eye movement is in the direction of the foveal flow and 1 when the current eye movement is in the direction of the previous eye movement. PDI index was evaluated for each full slow phase and then separately for the initial 40 ms of each slow phase. Shown in *A* are the distributions of PDI indexes for expansion and contraction stimuli for the full phases and for only the initial 40 ms (n = 2,415 for expansion, 1,535 for contraction).

compromise between the tendency to continue with the preceding slow phase direction and the need to follow the new direction of the stimulus motion. Thus there is evidence that the new eye movement direction that will be necessary after the gaze has shifted is calculated from the flow field position before the saccade and added onto the preceding eye movement direction.

Retinal flow fields

One aim of this study was to get an idea of typical flow fields on the retina during performance of unrestrained eye movements during optic flow stimulation. Of major interest in this regard are slow phase eye movements. The effect of a saccade on the retinal projection of the optic flow is mainly an offset or shift of the full visual image. In contrast, slow eye movements superimpose additional retinal motion onto the optic flow, resulting in a disturbance of the structure of the retinal flow field. The retinal projection of the optic flow field depends on direction and speed of the eye movement. Two extreme cases might illustrate this (Fig. 17, *A* and *B*). If the eye would be entirely stationary, the optic flow pattern would be projected onto the retina in a one-to-one manner. The retinal flow would retain a radial structure, and the focus of expansion immediately would indicate the direction of heading (Fig. 17*A*). In contrast, if the eyes were to perfectly track an individual element of the flow field, the resulting retinal flow would exhibit a singularity with spiraling motion around the fovea. Because the eye movement exactly cancels the flow field motion on the fovea, the fovea would remain without retinal slip during the eye movement (Fig. 17*B*). But the focus of expansion would be obscured because of the additional retinal motion induced by the eye movement.

We found both the speed and the direction of the eye movement to be related to the direction and speed of the foveated part of the flow field. Our major results in this regard were twofold. First, the directional differences between the foveal flow vector and the eye movement were small. Second, the gain, i.e., the ratio between the speed of the foveal motion and the speed of the eye, was low, ~0.45. This was especially pronounced in the most natural of our stimuli, the straight ahead motion on a ground plane. This means that the retinal flow field will neither be consistent with the flow field during constant gaze angle (Fig. 17*A*) nor will it be consistent with a flow field when the observer perfectly tracks (Fig. 17*B*). Instead, the retinal flow during slow phase eye movements will rather be in between these two conditions. This means, for example, that the singular point will neither be in the self-motion direction (as for constant gaze direction) nor will it be on the fovea (which is the case for perfect tracking movements). The singular point rather lies between those two points (Fig. 17*C*) and, depending on the momentary gain of the eye movement, shifts more to the heading direction or to the fovea.

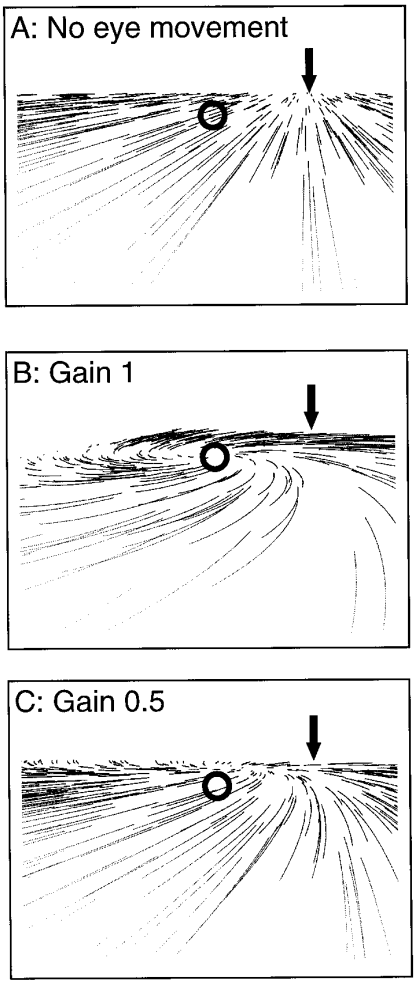

FIG. 17. Retinal flow fields during combined observer motion and eye movements in a ground plane environment. Because eye-movement–induced retinal slip is combined with the optic flow field on the retina, retinal flow differs from optic flow. Difference depends on the parameters of the eye movement. Direction of heading (→) and the direction of gaze (○) are the same in all 3 panels. *A* and *B*: retinal flow predicted from different assumptions about the eye movement. *A*: retinal flow under the assumption that no eye movements occur. *B*: retinal flow under the assumption of perfect foveal tracking of a flow field element. *C*: retinal flow for typical values of eye movement direction and speed that were observed in this study.

DISCUSSION

The observed pattern of alternating saccades and slow phases is typical for many situations in which scenes consisting of several objects are presented. The observer shifts gaze to different parts of the stimulus to scan details of the visual scene or look at and pursue objects to which the attention or interest is directed. A similar alternation of slow and fast eye movement phases is observed during optokinetic nystagmus. Several observations, which we will discuss later, suggest that the eye movements we observed are driven mainly by the optokinetic system.

In our experimental situation, the animal was not required to perform any task or to attend to any specific property or part of the stimulus. Therefore, attentive smooth pursuit would not necessarily be expected. Typically, attentive smooth pursuit leads to very irregular alternations of saccades with long- or short-lasting tracking phases. This was not observed. Instead, the duration of the slow phases and the regularity of the alternation between saccades and slow phases is more reminiscent of optokinetic nystagmus. For smooth pursuit, because of the generally low gain, a substan-

tial number of catch-up saccades would be expected to bring the tracked target back on the fovea. This was not the case. Therefore we have to regard the eye movements as, at least in part, to be elicited passively by retinal slip that occurs in optic flow fields whenever the gaze deviates from the focus of expansion. Two additional observations point toward an involvement of the optokinetic system. First, the systematic deviation of eye movement direction from the local flow field direction on the fovea (Fig. 8) argues for an integration of surrounding motion vectors. Such a global integration is typical for the optokinetic system. Second, the optokinetic system would be expected to show a low gain because the stimulus is suboptimal for OKN because of diverging flow field vectors within the visual field. In the next section, we will discuss specific properties of oculomotor responses to optic flow stimulation and relate them to properties of the optokinetic system.

Distribution of gaze positions

One of the first questions when one considers unrestrained visual inspection of optic flow fields is whether the eye is directed toward the focus of expansion. Although psychophysical experiments in humans show that it is not necessary to shift the eyes into the FOE to evaluate the direction of heading (Warren et al. 1988), heading detection is more accurate when the FOE is near the fovea (Warren and Kurtz 1992). Therefore, one might expect a ''natural'' tendency to shift the eyes into the FOE. Such a tendency has been described for humans during car driving (Mourant et al. 1969). In our monkeys, we did find a small shift of median eye position toward the FOE. However, contraction stimuli yielded a shift in the opposite direction. Moreover, the median gaze direction was affected strongly by head position; the shift of the median gaze direction was the same as the change in head direction. This suggest that median eye position is referenced to the zero position of the eyes in the head, i.e., the naso-temporal axis.

The opposite shifts for expansion and contraction might be consistently interpreted in relation to optokinetic nystagmus. During OKN, the average eye position (the Schlagfeld) is shifted against the direction of the stimulus motion (Jung and Mittermaier 1939). Similarly, median eye position in our experiments shifted against the global resultant motion of the stimulus when the FOE was eccentric. This motion is away from the FOE for expansion stimuli and toward the FOE for contraction stimuli. It has been suggested that the Schlagfeld in OKN serves to orient average eye position toward the direction of rotational self-movement (Bähring et al. 1994). Similarly, for simulated forward motion, the Schlagfeld shifts mean gaze direction toward the FOE. However, this shift is far from complete. Eye position on average deviates from the position of the FOE.

Properties of the slow phase eye movements and their stimulus specificity

Slow phase eye movements followed the direction of local stimulus motion on the fovea very precisely. The variability of directional differences, i.e., the angular deviation was smaller for contraction than for expansion and decreased for increasing eccentricity of the FOE and increasing observer speed. Several factors may account for this. First, the direction of the foveal flow may be determined faster and more accurately when its speed is high. Support for this view comes from psychophysical studies in humans (Mateeff et al. 1995) and from neurophysiology, because in motion processing areas MT and MST, the latency of the neuronal response decreases with increasing speed of the motion stimulus (Kawano et al. 1994; Lagae et al. 1994). A related effect could occur when the FOE becomes eccentric. In this case, the median distance between the fovea and the FOE increases, resulting in increased speed of the foveal motion. Second, a greater distance between the gaze direction and the FOE results in an more homogeneous flow field around the fovea. More homogeneous motion also might lead to greater directional alignment between stimulus direction and eye movement.

A striking finding was that the median gain was quite low, much lower than the typical gain of smooth pursuit or optokinetic eye movements. A direct comparison is difficult, first of all because we did not require the animals to pursue and second because our gain measure differs from standard measures for pursuit and OKN gain. We defined the gain with respect to the foveal flow, which in turn was determined from the measurement of eye position. Also, we had to calculate the gain for an accelerated movement by averaging gain values from individual data points. Yet, while a direct comparison is difficult, we have to accept and discuss the fact that the gain during optic flow stimulation is lower than the gain observed with full-field uniform motion, i.e., typical OKN stimulation.

Because motion directions in radial optic flow fields are not parallel, the gain might be reduced by inhibitory influences from opposing motion directions. In humans, OKN gain, and to a lesser degree also pursuit gain, are reduced in the presence of transparent motion in opposite directions (Niemann et al. 1994).

The optokinetic system is known to integrate visual motion signals from throughout the visual field. Especially important are the fovea and a parafoveal area of about 5 or 10° eccentricity. In the preceding text, we have defined the gain with respect to the foveal flow. But the input for the optokinetic system would more likely consist of the spatial average of motion signals from the fovea and parafovea. We therefore need to consider the consequences of such spatial averaging. In the APPENDIX, we derive an equation for the spatial average of motion signals within a given parafoveal region in the ground plane environment. The averaged motion signal usually has a substantially smaller speed than the foveal motion. Therefore, the low gain that we observed in comparison with the foveal motion might be explained from such an integration process in the optokinetic pathway. However, this is difficult to quantify because the averaged motion signal depends strongly on the exact size and shape of the integration area. However, we roughly estimated the effect in the following way. We assumed an integration of visual motion in an area of $\pm 10°$ around the fovea. Then we calculated the ratio between the averaged motion signal and the foveal motion for the average eye position during each slow phase. The median of this ratio across all slow phases was ~ 0.7. Therefore, on average the optokinetic input is only

70% of the foveal motion. Together with the observation that the typical gain of the optokinetic response in our monkeys is ~0.8, such an integration could explain the low values of the gain we observed with the optic flow stimuli.

We observed a consistent difference in gain between expansion and contraction. A combination of the accelerating and decelerating motion characteristics in these stimuli with the latencies in the visual system could be partially responsible for this. Visual motion signals reach the eye movement generators in the brain with a latency of ≥50 ms (Kawano et al. 1994; Miles et al. 1986). In contrast, our evaluation of the gain is based on a momentary comparison of eye speed with an idealized flow field speed assumed to occur at the recorded gaze position at the time of measurement. Because of visual latency, the signal that drives the eye movement is actually based on an earlier measurement of the flow field speed, potentially mismatching the current flow field speed. If we adjusted the procedure for the calculation of the gain to visual latency, the gain for expansional stimuli would be higher because the individual dots accelerate. For contractional stimuli, the gain would be lower because the individual dots decelerate. However, calculations of the effects of latency on the gain in these cases reveal that latencies ≤100 ms could account only for <20% of the observed differences. Thus there must be other mechanisms responsible for the different gain in expansion and contraction stimuli.

A connection to OKN could offer a potential explanation due to directional biases in the NOT and AOS which are not present in the DLPN, i.e., the smooth pursuit pathway. Left and right NOT take complementary roles in the generation of OKN. Each contains only neurons selective for ipsiversive visual motion and hence drives only ipsiversive slow eye movements (Hoffmann et al. 1988). Leftward slow phases of the OKN are driven by the left NOT, rightward by the right NOT. Each NOT has its maximum sensitivity for local visual motion in the parafoveal visual field. But in addition each NOT receives visual information from almost the entire contralateral visual hemifield field, but only from a strip of ~20–30° from the vertical meridian into the ipsilateral hemifield (Hoffmann et al. 1992). Even in the most sensitive parafoveal region, motion in the contralateral field yields stronger responses than motion in the ipsilateral field (Hoffmann et al. 1992). Now let us consider a situation where the direction of gaze is to the left of the FOE such as in Fig. 17*A*. Based on the gaze direction (Fig. 17*A*, ○) the flow field is split into two hemifields. The left hemifield contains largely homogeneous motion directions. The right hemifield contains the FOE and therefore a radial pattern with many different motion directions. If the motion on the screen were a contraction, the appropriate eye movement would be directed rightward, i.e., toward the focus of contraction. Such rightward eye movement would be driven by the right NOT. The major input to the right NOT comes from the fovea and the left visual hemifield. The left hemifield contains the peripheral part of the flow stimulus, in which motion is largely homogeneous. It provides an adequate stimulus for the right NOT, resulting in high eye velocity. For expansion the input to the NOT is weaker. The appropriate eye movement would be away from the FOE, i.e., toward the left in Fig. 17*A*. Leftward optokinetic eye movements are driven by the left NOT, which in turn receives its major input from the right visual hemifield. But the right visual hemifield contains the FOE, i.e., a radial motion pattern that contains many different motion directions and thus provides a weak or even suppressive input to the NOT. Hence, the resulting eye movement should be slower and exhibit a lower gain.

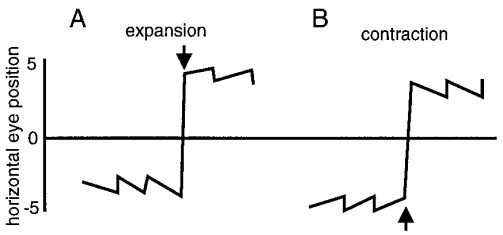

FIG. 18. Schematic illustration of the consequences of a saccade crossing the horizontal meridian for expansion (*A*) and contraction (*B*). When a saccade crosses the meridian, for expanding stimuli the eye movement direction after the saccade is in the same direction as the saccade itself. This is not the case for contraction.

Dynamic properties during the initial slow phase

With each saccade, the direction and speed of the foveal flow changes. Appropriate parameters for the eye movement after the saccade can be determined from foveal vision only after a delay of several tens of milliseconds due to the latency of the visual neurons. On the other hand, the parameters might in principle be obtained from peripheral vision already during the preceding slow phase. This would require a complex preprogramming of the slow eye movement before the saccade. For contraction, an initially good directional following was observed, which might be consistent with such a preprogramming. However, for expansion, the initial deviation is biased strongly toward the direction of the preceding slow phase eye movement. This would argue against such a preprogramming of the new eye movement direction or at least for an incomplete version of it.

There might be a different explanation for the large difference of initial angular deviation and gain between expanding and contracting stimuli and for the much higher initial deviation during expansion when the subsequent flow direction changed. For expansion, a saccade that crosses the horizontal position of the focus results in the interruption of a typical optokinetic behavior. During OKN, slow phases and saccades are oppositely directed. But during optic flow stimulation, when an approximately horizontal saccade crosses the FOE, the foveal motion direction is reversed. This is illustrated in Fig. 18. For expansion, the next slow eye movement direction after the saccade is in the same, or almost the same, direction as the saccade itself. This leads to the reversal of retinal slip direction only after the saccade. This is an unusual situation for the optokinetic system. It might require the acquisition of new visual information about the stimulus movement and lead to the observed initial angular deviation and lower gain. For contraction on the other hand, the direction of the slow phase after the saccade is opposite from the direction of the saccade crossing the FOE, similar to the situation during OKN. The interruption of the normal optokinetic behavior, in the case of contraction therefore occurs

before the saccade. This presaccadic deviation from the regular OKN scheme may be voluntarily initiated. After the saccade, the eye then can continue the expected OKN scheme because the subsequent eye movement direction will be opposite to the direction of the saccade.

Comparison with eye movements during real self-motion

Our experiments also need to be discussed with respect to eye movements occurring during real self-motion. In that case, the translational vestibulo-ocular reflex also would lead to eye movements that compensate for observer motion and tend to stabilize gaze on environmental targets (Paige and Tomko 1991b; Schwarz et al. 1989; Solomon and Cohen 1992).

Studies of eye movements during real forward observer movement found qualitatively similar behavior, because eye movement speed and direction depended on gaze direction relative to the path of motion (Paige and Tomko 1991a; Solomon and Cohen 1992; Tomko and Paige 1992). However, during real observer movement, the gain of the eye movement might be higher. Studies in walking monkeys suggest that gaze compensation in this situation is very good (Solomon and Cohen 1992). Several mechanisms might contribute to this. For instance, better gaze stabilization might have be obtained through attentive pursuit mechanisms when particular targets of interest are present (Solomon and Cohen 1992). The activity state of the animals, which were engaged in active motion, might have a modulatory influence on reflectory gaze stabilization mechanisms. Also, during real self-motion, additional visual information and other sensory signals could activate the oculomotor system more precisely. Stereoscopic depth, which our optic flow stimuli lacked, could enhance the gain by suppressing conflicting visual input originating from different depth planes (Busettini et al. 1996; Howard and Simpson 1989). Somatosensory feedback from leg muscle proprioceptors during walking also could have an influence. Moreover, the vestibulo-ocular reflex (VOR) also would be active. Input from the labyrinth organs during head rotation very directly lead to compensatory eye movements, the rotational vestibulo-ocular-reflex (RVOR). Also during linear acceleration of the head, primates exhibit compensatory eye movements (translational VOR, TVOR) within a specific frequency range (Paige and Tomko 1991b). As for the eOKN, the TVOR is dependent on the viewing distance or vergence of the eyes (Schwarz et al. 1989). During real egomotion, the TVOR could not only compensate the short-lasting rapid changes in head distance from the ground but also, by integration, use the head velocity to support the optokinetic system that is activated by the pure visual flow field stimuli as shown in our experiments. Miles (1994) emphasizes the close anatomic-functional-evolutionary relationship of eOKN and TVOR. The combination of several eye movement generation mechanisms may lead to a better stabilization of gaze on target, i.e., to a higher gain.

Relationship to neurophysiology

An essential part of the slow eye movement system driving pursuit and OKN is formed by areas MT and MST (Dürsteler and Wurtz 1988; Erickson and Dow 1989; Hoffmann et al. 1992; Kawano et al. 1994; Komatsu and Wurtz 1988). Area MST also contains neurons that respond to optic flow stimuli (Duffy and Wurtz 1991; Lappe et al. 1996; Tanaka and Saito 1989). Therefore, eye movements in response to optic flow stimulation also might be driven in part by area MST. But the relationship between eye movements and optic flow is mutual because optic flow analysis also requires to take eye movements into account. Area MST receives nonvisual feedback during the execution of smooth pursuit (Erickson and Thier 1991; Ilg and Thier 1997; Newsome et al. 1988) that might be used for the analysis of optic flow during eye movements (Bradley et al. 1996; Duffy and Wurtz 1994; Lappe 1997; Lappe et al. 1994).

The eye movements we observed here lead to a specific structure of the retinal flow pattern that resembles a spiralling motion. Neurons in MST also often respond to spiralling optic flow patterns (Duffy and Wurtz 1997; Graziano et al. 1994). This specificity could reflect a sensitivity for the patterns of retinal flow experienced during natural oculomotor behavior.

Retinal flow fields and ecological considerations

The retinal motion pattern flow during forward movement is a combination of radial optic flow with retinal slip induced by eye movement. Estimation of the direction of heading could be based on the pattern of the flow (Gibson 1950; Warren and Hannon 1990) or involve an extraretinal eye movement signal (Banks et al. 1996; Royden 1994; Royden et al. 1994; Sperry 1950; Von Holst and Mittelstaedt 1950). Accurate visual-only heading detection is possible when eye movements stabilize gaze onto a specific element of a ground plane (van den Berg 1993; Warren and Hannon 1990) or when eye movements are slow [$<1-2°$ (Banks et al. 1996; Royden et al. 1994; Warren and Hannon 1990), $<6°$ (van den Berg 1993)]. The spontaneous eye movements in our study were mostly consistent with the requirements for visual heading detection. Median eye velocity during expansion did not exceed 6.2°/s. Eye movement direction followed the motion of elements of the flow field. However, eye speed accounted for only ~50% of the speed of the foveal motion. This could reflect a compromise between the requirements of retinal image stabilization and optic flow analysis. During perfect stabilization the singular point is always on the fovea. However, for the analysis of optic flow, the singular point provides a robust, easily detectable feature. If located on the fovea, its use in gaining information for self-motion would be limited. But if no eye movements are performed fast visual motion on the fovea impairs accurate image processing. A possible compromise lies in matching the direction of the foveal motion but not its speed. This keeps retinal flow structure to some degree while simultaneously reducing retinal slip on the fovea.

The observation that direction and speed of the eye movement follow the flow to different extents has implications for mechanisms of heading detection from optic flow. The strong directional correlation could be exploited in two ways. First, it could be used as a constraint in the purely visual analysis of retinal flow, which reduces the number of degrees of freedom (Lappe and Rauschecker 1993; Perrone and

Stone 1994). Second, it could be used in a scheme based on extraretinal feedback. The eye movement already provides a cue about the direction of heading because it is directed along a line away from the FOE. However, the placement of the direction of heading on this line is less well determined as it depends on the highly variable gain. It would have to be evaluated by a more complex visual mechanism.

In conclusion, we have shown that radial optic flow induces optokinetic eye movements. These eye movements are linked to the optic flow occurring around the direction of gaze. This suggests that such eye movements commonly occur even without a voluntary intention to pursue as soon as the eyes deviate from the focus of expansion. Therefore, mechanisms of optic flow processing have to deal with the presence of such involuntary eye movements.

APPENDIX

The optokinetic system is known to integrate motion signals from an extended part of the visual field. In this appendix, we want to determine the consequences of such an integration or averaging of motion signals. In the definition of parameters such as the gain or the angular difference, we have used the foveal flow as a reference. Here we will calculate the motion signal that is derived from the optic flow when visual motion is averaged in a larger parafoveal area.

We start out with *Eq. 5*, which describes the visual motion $\mathbf{f}$ at each point (x, y) on the tangent screen. Because $T_Y = 0$ in our stimuli, *Eq. 5* becomes

$$\mathbf{f}(x, y) = \frac{y}{0.47h}\begin{pmatrix} 0.47T_X - xT_Z \\ -yT_Z \end{pmatrix}$$

We are now interested in averaging the motion within a certain screen area. For convenience we will use a rectangular area extending from $(x - \Delta x, y - \Delta y)$ to $(x + \Delta x, y + \Delta y)$. The average motion in this area is given by

$$\hat{\mathbf{f}}(x, y, \Delta x, \Delta y) = \frac{\int_{x-\Delta x}^{x+\Delta x}\int_{y-\Delta y}^{y+\Delta y} D(x', y')\mathbf{f}(x', y')\mathrm{d}x'\mathrm{d}y'}{\int_{x-\Delta x}^{x+\Delta x}\int_{y-\Delta y}^{y+\Delta y} D(x', y')\mathrm{d}x'\mathrm{d}y'} \quad (A1)$$

where $D(x', y')$ is the density of the visible dots on the screen. This density varies across the screen. It is highest near the horizon and lowest in the bottom part of the screen. It can be calculated from the density of points on the ground plane in the following way. Because we used equally distributed random dots on the ground plane, their density is just some constant number D_0. We now want to know the density at point (x, y) on the screen. We assume an infinitesimal area A on the ground plane that is projected onto an area a around (x, y) on the screen. The density on the screen is then

$$D(x, y) = D_0\frac{A}{a}$$

Let A be the rectangular area enclosed by $(X, -h, Z)$ and $(X + \Delta X, -h, Z + \Delta Z)$. Hence

$$A = \Delta X\Delta Z$$

Because of *Eq. 1*, these points will be projected onto points $0.47(X/Z, -h/Z)$ and $0.47[(X + \Delta X)/(Z + \Delta Z), -h/(Z + \Delta Z)]$, respectively. The area enclosed by these points on the screen is

$$a = 0.47^2\left(\frac{X + \Delta X}{Z} - \frac{X}{Z}\right)\left(\frac{-h}{Z + \Delta Z} - \frac{-h}{Z}\right)$$

$$= 0.47^2\left(\frac{\Delta X}{Z}\right)\left(\frac{h\Delta Z}{Z^2 + Z\Delta Z}\right)$$

$$= 0.47^2\frac{h\Delta X\Delta Z}{Z^3 + Z^2\Delta Z}$$

The density on the screen is therefore

$$D(x, y) = D_0\frac{1}{0.47^2}\frac{Z^3 + Z^2\Delta Z}{h}$$

and with $\Delta Z \to 0$

$$D(x, y) = D_0\frac{1}{0.47^2}\frac{Z^3}{h}$$

With *Eq. 1* and $Y = -h$, we can express Z by the screen coordinate y as

$$Z = 0.47\frac{-h}{y}$$

Therefore, the density on the screen can finally be expressed as

$$D(x, y) = -0.47D_0\frac{h^2}{y^3} \quad (A2)$$

We now can proceed to calculate the average motion within the area between $(x - \Delta x, y - \Delta y)$ and $(x + \Delta x, y + \Delta y)$ on the screen

$$\int_{x-\Delta x}^{x+\Delta x}\int_{y-\Delta y}^{y+\Delta y} D(x', y')\mathbf{f}(x', y')\mathrm{d}x'\mathrm{d}y'$$

$$= D_0h\int_{x-\Delta x}^{x+\Delta x}\int_{y-\Delta y}^{y+\Delta y}\frac{1}{y'^2}\begin{pmatrix} -0.47T_X + x'T_Z \\ y'T_Z \end{pmatrix}\mathrm{d}x'\mathrm{d}y'$$

$$= 2D_0h\Delta x\int_{y-\Delta y}^{y+\Delta y}\frac{1}{y'^2}\begin{pmatrix} -0.47T_X + xT_Z \\ y'T_Z \end{pmatrix}\mathrm{d}y'$$

$$= 2D_0h\Delta x\begin{bmatrix} \left(\frac{1}{y - \Delta y} - \frac{1}{y + \Delta y}\right)(-0.47T_X + xT_Z) \\ \ln\left(\frac{y + \Delta y}{y - \Delta y}\right)T_Z \end{bmatrix}$$

$$\int_{x-\Delta x}^{x+\Delta x}\int_{y-\Delta y}^{y+\Delta y} D(x', y')\mathrm{d}x'\mathrm{d}y'$$

$$= -0.47D_0h^2\int_{x-\Delta x}^{x+\Delta x}\int_{y-\Delta y}^{y+\Delta y}\frac{1}{y'^3}\mathrm{d}x'\mathrm{d}y'$$

$$= -0.47D_0h^2\Delta x\left[-\frac{1}{(y + \Delta y)^2} + \frac{1}{(y - \Delta y)^2}\right]$$

$$= -0.47D_0h^2\Delta x\left(\frac{1}{y - \Delta y} + \frac{1}{y + \Delta y}\right)\left(\frac{1}{y - \Delta y} - \frac{1}{y + \Delta y}\right)$$

Therefore, the averaged motion is

$$\hat{\mathbf{f}}(x, y, \Delta x, \Delta y) = \frac{2}{0.47h}\left(\frac{1}{y - \Delta y} + \frac{1}{y + \Delta y}\right)^{-1} \times \begin{bmatrix} -0.47T_X + xT_Z \\ \left(\frac{1}{y - \Delta y} - \frac{1}{y + \Delta y}\right)^{-1}\ln\left(\frac{y + \Delta y}{y - \Delta y}\right)T_Z \end{bmatrix} \quad (A3)$$

This equation describes the average motion signal from an area extending $\pm\Delta x$ horizontally and $\pm\Delta y$ vertically from the direction

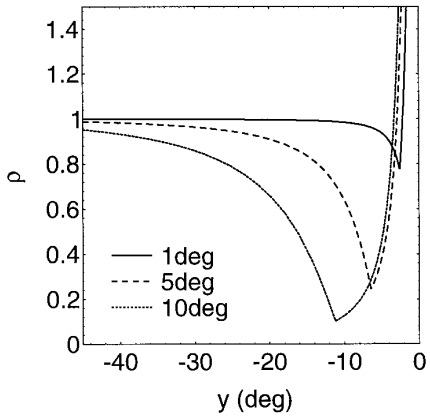

FIG. A1. Effects of spatial averaging of motion signals in a parafoveal integration area. Shown is the speed of the averaged motion in proportion of the speed of the foveal motion ($\rho = \hat{f}/f$) as a function of the vertical position y along the meridian of the screen ($x = 0$). Three different integration areas were used, ± 1, ± 5, or $\pm 10°$.

of gaze (x, y). However, because the ground plane in our stimuli was truncated 1.6° below the horizon, we have to modify the above equation when the upper limit of the integration field exceeds this border. In that case, $y + \Delta y$ has to be replaced by $y_{\max} = -1.6°$.

We now can compare the averaged motion within a given parafoveal area to the motion in the direction of gaze, i.e., the foveal flow that we have used for instance in the definition of the gain. We define the ratio between the motion averaged across a certain parafoveal region and the foveal motion as

$$\rho(x, y, \Delta x, \Delta y) = \frac{\|\hat{\mathbf{f}}(x, y)\|}{\|\mathbf{f}(x, y)\|}$$

This ratio depends on the size of the region over which motion is to be averaged and also on the position (x, y). Figure A1 shows the dependence of ρ on the vertical position y for three different integration regions, $\Delta x = \Delta y = 1, 5, 10°$. It is apparent that the averaged parafoveal motion is usually much smaller than the foveal motion ($\rho < 1$). This means that a spatial averaging of motion signals around the fovea results in a reduction of the motion input. Note, however, that this depends on position. For positions near the visible horizon ($y > -3°$), ρ is >1, meaning that spatial averaging results in an stronger motion signal. The reason for this is that the integration area becomes asymmetric, as motion signals above the visible horizon are missing.

We are indebted to Drs. Frank Bremmer, Alexander Thiele, and Tobias Niemann for help with the experiments and for carefully reading various versions of the manuscript.

This research was supported by the Deutsche Forschungsgemeinschaft (La 952/1-1 and SFB 509) and the Human Frontier Science Program.

Address reprint requests to M. Lappe.

Received 20 June 1997; accepted in final form 13 December 1997.

REFERENCES

BÄHRING, R., MEIER, R. K., AND DIERINGER, N. Unilateral ablation of the frontal eye field of the rat affects the beating field of ocular nystagmus. *Exp. Brain Res.* 98: 391–400, 1994.

BANKS, M. S., EHRLICH, S. M., BACKUS, B. T., AND CROWELL, J. A. Estimating heading during real and simulated eye movements. *Vision Res.* 36: 431–443, 1996.

BRADLEY, D., MAXWELL, M., ANDERSEN, R., BANKS, M. S., AND SHENOY, K. V. Mechanisms of heading perception in primate visual cortex. *Science* 273: 1544–1547, 1996.

BREMMER, F., DISTLER, C., AND HOFFMANN, K.-P. Eye position effects in monkey cortex. II. Pursuit and fixation related activity in posterior parietal areas LIP and 7A. *J. Neurophysiol.* 77: 962–977, 1997.

BUSETTINI, C., MASSON, G., AND MILES, F. A role for stereoscopic depth cues in the rapid visual stabilization of the eyes. *Nature* 380: 342–345, 1996.

COHEN, B., MATSUO, V., AND RAPHAN, T. Quantitative analysis of the velocity characteristics of optokinetic nystagmus and optokinetic after-nystagmus. *J. Physiol. (Lond.)* 270: 321–344, 1977.

DUFFY, C. J. AND WURTZ, R. H. Sensitivity of MST neurons to optic flow stimuli. I. A continuum of response selectivity to large-field stimuli. *J. Neurophysiol.* 65: 1329–1345, 1991.

DUFFY, C. J. AND WURTZ, R. H. Optic flow responses of MST neurons during pursuit eye movements. *Soc. Neurosci. Abstr.* 20: 1279, 1994.

DUFFY, C. AND WURTZ, R. Planar directional contributions to optic flow responses in MST neurons. *J. Neurophysiol.* 77: 782–796, 1997.

DÜRSTELER, M. R. AND WURTZ, R. H. Pursuit and optokinetic deficits following chemical lesions of cortical areas MT and MST. *J. Neurophysiol.* 60: 940–965, 1988.

ERICKSON, R. G. AND DOW, B. M. Foveal tracking cells in the superior temporal sulcus of the macaque monkey. *Exp. Brain Res.* 78: 113–131, 1989.

ERICKSON, R. G. AND THIER, P. A neuronal correlate of spatial stability during periods of self-induced visual motion. *Exp. Brain Res.* 86: 608–616, 1991.

GIBSON, J. J. *The Perception of the Visual World.* Boston: Houghton Mifflin, 1950.

GOTTLIEB, J., MACAVOY, M., AND BRUCE, C. Neural responses related to smooth-pursuit eye movements and their correspondence with electrically elicited smooth eye movements in the primate frontal eye field. *J. Neurophysiol.* 72: 1634–1653, 1994.

GRAZIANO, M.S.A., ANDERSEN, R. A., AND SNOWDEN, R. Tuning of MST neurons to spiral motions. *J. Neurosci.* 14: 54–67, 1994.

HEEGER, D. J. AND JEPSON, A. Subspace methods for recovering rigid motion. I. Algorithm and implementation. *I. J. Comput. Vis.* 7: 95–117, 1992.

HOFFMANN, K.-P. Neuronal responses related to optokinetic nystagmus in the cat's nucleus of the optic tract. In: *Progress in Oculomotor Research,* edited by A. Fuchs and W. Becker. Amsterdam: Elsevier, 1981, p. 443–454.

HOFFMANN, K.-P. Responses of single neurons in the pretectum of monkeys to visual stimuli in three dimensional space. *Ann. NY Acad. Sci.* 545: 180–186, 1988.

HOFFMANN, K.-P. AND DISTLER, C. Quantitative analysis of visual receptive fields of neurons in nucleus of the optic tract and dorsal terminal nucleus of the accessory optic tract in macaque monkey. *J. Neurophysiol.* 62: 416–427, 1989.

HOFFMANN, K.-P., DISTLER, C., ERICKSON, R. G., AND MADER, W. Physiological and anatomical identification of the nucleus of the optic tract and dorsal terminal nucleus of the accessory optic tract in monkeys. *Exp. Brain Res.* 69: 635–644, 1988.

HOFFMANN, K.-P., DISTLER, C., AND ILG, U. Callosal and superior temporal sulcus contributions to receptive field properties in the macaque monkey's nucleus of the optic tract and dorsal terminal nucleus of the accessory optic tract. *J. Comp. Neurol.* 321: 150–162, 1992.

HOWARD, I. P. AND SIMPSON, W. A. Human optokinetic nystagmus is linked to the stereoscopic system. *Exp. Brain Res.* 78: 309–314, 1989.

ILG, U. J. AND THIER, P. MST neurons are activated by pursuit of imaginary targets. In: *Parietal Lobe Contributions to Orientation in 3D-Space,* edited by P. Thier and H.-O. Karnath. Berlin: Springer, 1997, p. 173–184.

JUNG, R. AND MITTERMAIER, R. Zur objektiven Registrierung und Analyse verschiedener Nystagmusformen: Vestibulärer, optokinetischer und spontaner Nystagmus in ihren Wechselbeziehungen. *Arch. Ohren-Nasen-Kehlkopf-Heilkunde* 146: 410–439, 1939.

KAWANO, K. AND MILES, F. A. Short-latency ocular following responses of monkey. II. Dependence on a prior saccadic eye movement. *J. Neurophysiol.* 56: 1355–1380, 1986.

KAWANO, K., SHIDARA, M., WATANABE, Y., AND YAMANE, S. Neural activity in cortical area MST of alert monkey during ocular following responses. *J. Neurophysiol.* 71: 2305–2324, 1994.

KAWANO, K., SHIDARA, M., AND YAMANE, S. Neural activity in dorsolateral pontine nucleus of alert monkey during ocular following responses. *J. Neurophysiol.* 67: 680–703, 1992.

KAWANO, K., TAKEMURA, A., INOUE, Y., KITAMA, T., KOBAYASHI, Y., AND

MUSTARI, M. J. Visual inputs to cerebellar ventral paraflocculus during ocular following responses. *Prog. Brain Res.* 112: 415–422, 1996.

KELLER, E. AND KAHN, N. S. Smooth-pursuit initiation in the presence of a textured background in the monkey. *Vision Res*. 26: 943–955, 1986.

KOMATSU, H. AND WURTZ, R. H. Relation of cortical areas MT and MST to pursuit eye movements. I. Localization and visual properties of neurons. *J. Neurophysiol.* 60: 580–603, 1988.

LAGAE, L., MAES, H., RAIGUEL, S., XIAO, D.-K., AND ORBAN, G. A. Responses of macaque STS neurons to optic flow components: a comparison of areas MT and MST. *J. Neurophysiol.* 71: 1597–1626, 1994.

LAPPE, M. Analysis of self-motion by parietal neurons. In: *Parietal Lobe Contributions to Orientation in 3D-Space*, edited by P. Thier and H.-O. Karnath. Heidelberg: Springer Verlag, 1997, p. 597–618.

LAPPE, M., BREMMER, F., AND HOFFMANN, K.-P. How to use non-visual information for optic flow processing in monkey visual cortical area MSTd. In: *ICANN 94—Proceedings of the International Conference on Artificial Neural Networks, 26–29 May 1994, Sorrento,* edited by M. Marinaro and P. G. Morasso. Berlin: Springer, 1994, p. 46–49.

LAPPE, M., BREMMER, F., PEKEL, M., THIELE, A., AND HOFFMANN, K.-P. Optic flow processing in monkey STS: a theoretical and experimental approach. *J. Neurosci.* 16: 6265–6285, 1996.

LAPPE, M. AND RAUSCHECKER, J. P. A neural network for the processing of optic flow from ego-motion in man and higher mammals. *Neural Comp.* 5: 374–391, 1993.

LAPPE, M. AND RAUSCHECKER, J. P. Motion anisotropies and heading detection. *Biol. Cybern.* 72: 261–277, 1995.

LISBERGER, S. G. AND FUCHS, A. F. Role of primate flocculus during rapid behavioral modification of vestibulo-ocular reflex. I. Purkinje cell activity during visually guided horizontal smooth pursuit eye movement and passive head rotation. *J. Neurophysiol.* 41: 733–763, 1978.

LISBERGER, S. G. AND WESTBROOK, L. E. Properties of visual inputs that initiate horizontal smooth pursuit eye movements in monkeys. *J. Neurosci.* 5: 1662–1673, 1985.

LONGUET-HIGGINS, H. C. AND PRAZDNY, K. The interpretation of a moving retinal image. *Proc. R. Soc. Lond. B Biol. Sci.* 208: 385–397, 1980.

MATEEFF, S., DIMITROV, G., AND HOHNSBEIN, J. Temporal thresholds and reaction time to changes in velocity of visual motion. *Vision Res.* 35: 355–363, 1995.

MATSUO, V. AND COHEN, B. Vertical optokinetic nystagmus and vestibular nystagmus in the monkey: up down asymmetry and effects of gravity. *Exp. Brain Res.* 53: 197–216, 1984.

MILES, F. A. Stimulus specificity in the primate optokinetic system. In: *Information Processing Underlying Gaze Control*, edited by J. M. Delgado-Garcia, E. Godeux, and P.-P. Vidal. Oxford: Pergamon, 1994, p. 251–259.

MILES, F. A. AND BUSETTINI, C. Ocular compensation for self-motion. *Ann. NY Acad. Sci.* 656: 220–232, 1992.

MILES, F. A., KAWANO, K., AND OPTICAN, L. M. Short-latency ocular following responses of monkey. I. Dependence on temporospatial properties of visual input. *J. Neurophysiol.* 56: 1321–1354, 1986.

MOHRMANN, H. AND THIER, P. The influence of structured visual backgrounds on smooth-pursuit initiation, steady-state pursuit and smooth-pursuit termination. *Biol. Cybern.* 73: 83–93, 1995.

MOURANT, R. R., ROCKWELL, T. H., AND RACKOFF, N. J. Driver's eye movements and visual workload. *Highway Res. Rec.* 292: 1–10, 1969.

MURUSAGI, C. M. AND HOWARD, I. P. Up-down asymmetry in human vertical optokinetic nystagmus and afternystagmus: contributions of the central and peripheral retinae. *Exp. Brain Res.* 77: 183–192, 1989.

MUSTARI, M. J. AND FUCHS, A. F. Response properties of single units in the lateral terminal nucleus of the accessory optic system in the behaving primate. *J. Neurophysiol.* 61: 1207–1220, 1989.

NEWSOME, W. T., WURTZ, R. H., AND KOMATSU, H. Relation of cortical areas MT and MST to pursuit eye movements. II. Differentiation of retinal from extraretinal inputs. *J. Neurophysiol.* 60: 604–620, 1988.

NIEMANN, T., ILG, U. J., AND HOFFMANN, K.-P. Eye movements elicited by transparent stimuli. *Exp. Brain Res.* 98: 314–322, 1994.

PAIGE, G. D. AND TOMKO, D. L. Eye movement responses to linear head motion in the squirrel monkey. II. Visual–vestibular interactions and kinematic considerations. *J. Neurophysiol.* 65: 1184–1196, 1991a.

PAIGE, G. D. AND TOMKO, D. L. Eye movement responses to linear head motion in the squirrel monkey. I. Basic characteristics. *J. Neurophysiol.* 65: 1170–1183, 1991b.

PERRONE, J. A. AND STONE, L. S. A model of self-motion estimation within primate extrastriate visual cortex. *Vision Res.* 34: 2917–2938, 1994.

REGAN, D. AND BEVERLY, K. I. How do we avoid confounding the direction we are looking and the direction we are moving? *Science* 215: 194–196, 1982.

ROYDEN, C. S. Analysis of misperceived observer motion during simulated eye rotations. *Vision Res.* 34: 3215–3222, 1994.

ROYDEN, C. S., CROWELL, J. A., AND BANKS, M. S. Estimating heading during eye movements. *Vision Res.* 34: 3197–3214, 1994.

SAKATA, H., SHIBUTANI, H., AND KAWANO, K. Functional properties of visual tracking neurons in posterior parietal association cortex of the monkey. *J. Neurophysiol.* 49: 1364–1380, 1983.

SCHWARZ, U., BUSETTINI, C., AND MILES, F. A. Ocular responses to linear motion are inversely proportional to viewing distance. *Science* 245: 1394–1396, 1989.

SOLOMON, D. AND COHEN, B. Stabilization of gaze during circular locomotion in light: I. Compensatory head and eye nystagmus in the running monkey. *J. Neurophysiol.* 67: 1146–1157, 1992.

SPERRY, R. W. Neural basis of the spontaneous optokinetic response produced by visual inversion. *J. Comp. Physiol. Psychol.* 43: 482–489, 1950.

SUZUKI, D. A. AND KELLER, E. L. Visual signals in the dorsolateral pontine nucleus of the alert monkey: their relationship to smooth–pursuit eye movements. *Exp. Brain Res.* 53: 473–478, 1984.

TANAKA, K. AND SAITO, H.-A. Analysis of motion of the visual field by direction, expansion/contraction, and rotation cells clustered in the dorsal part of the medial superior temporal area of the macaque monkey. *J. Neurophysiol.* 62: 626–641, 1989.

THIER, P., KÖHLER, W., AND BÜTTNER, U. W. Neuronal activity in the dorsolateral pontine nucleus of the alert monkey modulated by visual stimuli and eye movements. *Exp. Brain Res.* 70: 496–512, 1988.

TOMKO, D. L. AND PAIGE, G. D. Linear vestibuloocular reflex during motion along axes between nasooccipital and interaural. *Ann. NY Acad. Sci.* 656: 233–241, 1992.

VAN DEN BERG, A. V. Perception of heading. *Nature* 365: 497–498, 1993.

VAN DEN BERG, A. V. Judgements of heading. *Vision Res.* 36: 2337–2350, 1996.

VAN DEN BERG, A. V. AND COLLEWIJN, H. Directional asymmetries of human optokinetic nystagmus. *Exp. Brain Res.* 70: 597–604, 1988.

VON HOLST, E. AND MITTELSTAEDT, H. Das Reafferenzprinzip (Wechselwirkung zwischen Zentralnervensystem und Peripherie). *Naturwissenschaften* 37: 464–476, 1950.

WARREN, W. H., JR. AND HANNON, D. J. Eye movements and optical flow. *J. Opt. Soc. Am. A* 7: 160–169, 1990.

WARREN, W. H., JR. AND KURTZ, K. J. The role of central and peripheral vision in perceiving the direction of self-motion. *Percept. Psychophys.* 51: 443–454, 1992.

WARREN, W. H., JR., MORRIS, M. W., AND KALISH, M. Perception of translational heading from optical flow. *J. Exp. Psychol. Hum. Percept. Perform.* 14: 646–660, 1988.